NUMBER 154 OCTOBER 2021

QN

Quaternary Newsletter

A publication of the
Quaternary Research Association

QUATERNARY NEWSLETTER

EDITOR:
Dr Sarah Woodroffe

Department of Geography, Durham University, Lower Mountjoy, South Road, Durham, DH1 3LE

(e-mail: s.a.woodroffe@durham.ac.uk

Instructions to authors

Quaternary Newsletter is issued in February, June and October. Articles, reviews, notices of forthcoming meetings, news of personal and joint research projects etc. are invited and should be sent to the Editor. Closing dates for submission of copy (news, notices, reports etc.) for the relevant issues are 5th January, 1st May and 1st September. These dates will be strictly adhered to in order to expedite publication. **Articles must be submitted at least 6 weeks before these dates in order to be reviewed and revised in time for the next issue of QN, otherwise they may appear in a subsequent issue.**

Suggested word limits are as follows: obituaries (2000 words); articles (3000 words); reports on meetings (2000 words); reports on QRA grants (800 words); reviews (1000 words); letters to the Editor (500 words); abstracts (500 words). Authors submitting work as Word documents that include figures must send separate copies of the figures in .eps, .tif or .jpg format (minimum resolution of 300 dpi is required for accurate reproduction). Quaternary Research Fund and New Researchers Award Scheme reports should limit themselves to describing the results and significance of the actual research funded by QRA grants. The suggested format for these reports is as follows: (1) background and rationale (including a summary of how the grant facilitated the research), (2) results, (3) significance, (4) acknowledgments (if applicable). The reports should not (1) detail the aims and objectives of affiliated and larger projects (e.g. PhD topics), (2) outline future research and (3) cite lengthy reference lists. No more than one figure per report is necessary. Recipients of awards who have written reports are encouraged to submit full-length articles on related or larger research projects

NB: Updated guidelines on the formatting of contributions are now available via the QRA webpage and from the editor.

Argraff/Printed by:
Gwasg Ffrancon Press
BETHESDA
Gwynedd, North Wales
Tel: 01248 601669 Fax: 01248 602634.

COVER PHOTOGRAPH

Digging up the past: 10 m high open-face exposure of Late Devensian glaciolacustrine sediments deposited at Hemingbrough, North Yorkshire.
Photo credit Simon Crowhurst.

ARTICLES

HEMINGBROUGH CHRONOSTRATIGRAPHY: HAVE BRITICE-CHRONO GOT IT RIGHT?

Della Murton

Quaternary Palaeoenvironments Group, University of Cambridge, Cambridge, CB2 3EN

della.murton@cantab.net

Introduction

The Vale of York is a sedimentary basin situated in central eastern England, infilled with up to up to 24 m of superficial sediments deposited during the Devensian glacial Stage (Gaunt *et al*., 1992; Gaunt, 1994; Ford *et al*., 2008). With regards to British Quaternary stratigraphy one important site in the region is Hemingbrough, situated in the central part of the vale, 5 km south east of Selby, North Yorkshire (Figure 1). This locality is the type site for the Hemingbrough Formation (Thomas, 1999), which constitutes most of the basin-fill sediments. In 2003 Officers of the British Geological Survey (BGS) re-mapped the Selby district, and in doing so recognised three constituent members of this formation. From the base upwards these are: Park Farm Member, Lawns House Farm Member and Thorganby Member (Ford *et al*., 2008). The Park Farm and Thorganby members comprise laminated to massive silty clays, whereas the Lawns House Farm Member comprises silty sand. From their mapping Ford *et al*. (2008) considered the Lawns House Farm Member to form a lobe extending and thinning southwards from the Escrick moraine ridge, which they considered represented the maximum limit of Late Devensian ice in the Vale of York. The southernmost extent of the Lawns House Farm Member was unknown due to a lack of field exposures in the Selby district. Hemingbrough, however, lies at the northern edge of the adjacent Doncaster geological map sheet and so was not mapped by Ford *et al*. (2008). Instead the revised lithostratigraphy from the Selby district was extrapolated by the BGS onto other geological map sheets covering the Vale of York, standardising the stratigraphical nomenclature and thus replacing the previous lithostratigraphical model of Gaunt (1994) for the region. The deposits respectively under- and overlying the Hemingbrough Formation in the central part of the Vale of York south of the Escrick moraine ridge are sands and gravels comprising the Basal Glaciofluvial Deposits, and sands of the Breighton Formation (Ford *et al*., 2008).

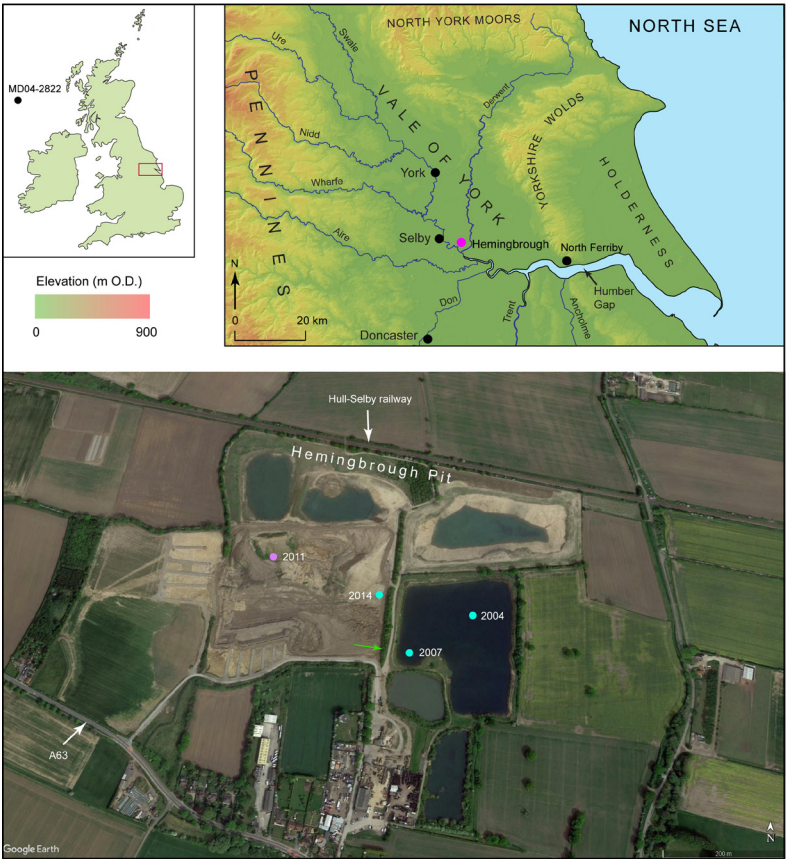

Figure 1. Site location of Hemingbrough and other places mentioned in the text. Dots on Google Earth image (taken 5/7/2020) show locations of open-face exposures and the core sampling site, with the year visited. Turquoise dots relate to Murton *et al*. (2009) and Murton (2017), pink dot to Bateman *et al*. (2015) and Evans *et al*. (2021).

This article will focus on the Hemingbrough Formation. The objectives are to (1) provide an overview of the lithostratigraphy and sedimentary properties, and (2) to develop three simple age models to assess the chronologies for deposition of the Hemingbrough sediments proposed by Murton *et al*. (2009) and BRITICE-CHRONO (Bateman *et al*., 2015, 2018; Evans *et al*., 2021). All descriptions, interpretations and data presented in the subsequent two sections are taken from the relevant cited paper. It is beyond the scope of this article to evaluate the palaeoenvironmental reconstructions presented by BRITICE-CHRONO for eastern England in relation to the age models proposed here.

Background to the Murton *et al.* (2009) chronology

Open-face exposures of the basin-fill sediments in the central part of the Vale of York are scarce, and Hemingbrough is one of only a few sites where the sediments can be accessed. That said, only the uppermost 10 m of sediment are exposed due a perched water table below this depth. The author first visited the Hemingbrough pit in 2004 (Figure 1), where she collected overlapping 0.5 m-long monoliths from steps mechanically excavated into the open-face exposure. Depths for each step were determined accurately using an engineer's level and staff. Three lithological units (HB1–HB3) were identified (Figure. 2A–B). From the base upwards these comprised (1) laminated clayey silt interbedded with massive to faintly stratified clayey silt (unit HB1; 5.6 m thick) (Figure. 2C), (2) massive silt with sandy interbeds or laminae (unit HB2; 3.3 m thick) (Figure. 2D–E). This is overlain by (3) laminated to massive clayey silt (unit HB3; 0.7–1.2 m thick). Symmetrical ripple form sets, interpreted as wave ripples, were observed both in plan and cross-section within the silty sand sediments (Figure. 2D–F). The presence of these sedimentary structures provided an exciting opportunity to pioneer whether such sediments could be dated by optically stimulated luminescence (OSL) as wave ripples form in shallow water depths (above wave base) which would result in a high propensity for adequate solar resetting of the OSL signal. Of five prominent silty sand beds recognised in the lithostratigraphy, numbered H1–H5, two were selected for dating (Figure. 2A). The author collected three samples from these silty sand beds in 2007 (Figure. 5). Two samples were collected from bed H1, at 4.0 m depth, and one from bed H4, at 1.5 m depth. These samples were processed in the luminescence laboratory at Royal Holloway, University of London with the results published in Murton *et al*. (2009).

As outlined in Murton *et al*. (2009), lithological units HB1–HB3 were assigned tentatively to the recently-revised lithostratigraphy of Ford *et al*. (2008). They noted that although the Hemingbrough sequence did not contain a single, thick sand layer directly comparable to the Lawns House Farm Member (as described in Ford *et al*. (2008)), the prominent sandy beds (numbered H1–5 in their unit HB2) were regarded as distal equivalents. At the time, they could not unequivocally discount the possibility that these sandy beds were part of the Park Farm Member.

Background to the Bateman *et al.* (2015) chronology

Bateman and co-authors visited Hemingbrough in 2011 (Figure. 1), where they logged a tripartite sedimentary sequence exposed in field section, which they attributed to the Hemingbrough Formation. They described their field exposure, from the base upwards, as the Park Farm Member (at least 10 m thick) comprised of laminated silt and clay; the Lawns House Farm Member (>1 m thick) comprised of wavy and convoluted laminations of sand and silty clay; and the Thorganby Member (1.8 m thick) comprised of massive silty clay coarsening upwards into

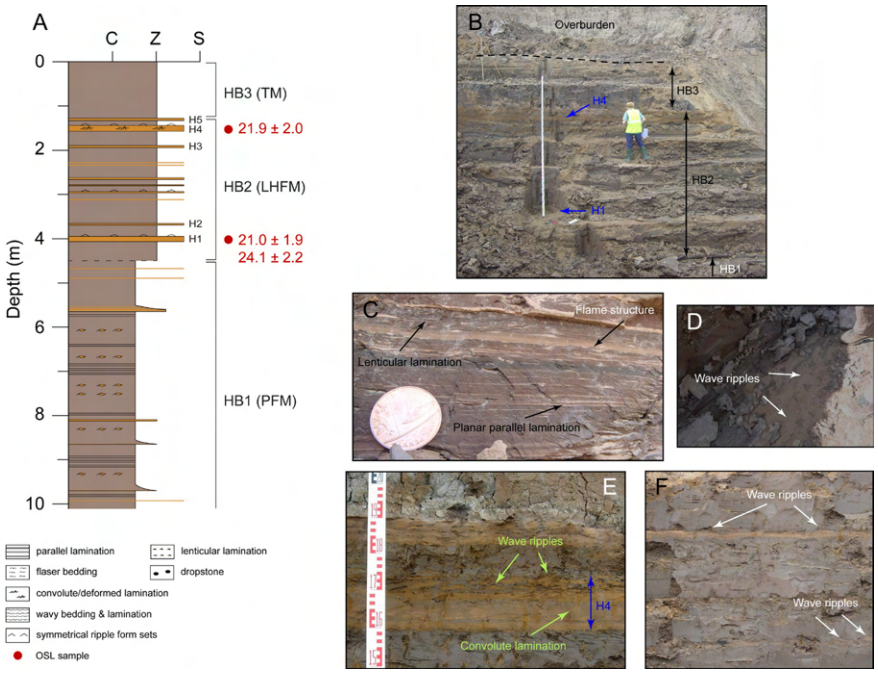

Figure 2. (A) Stratigraphic log for Hemingbrough from field observations and monoliths showing the dominant sedimentary structures. Lithostratigraphy from Ford *et al*. (2008). PFM: Park Farm Member; LHFM: Lawns House Farm Member; TM: Thorganby Member. OSL ages in red. (B) Open-face exposure in 2004, highlighting the location of OSL-dated silty sand beds H1 and H4. Photograph courtesy of Jim Rose. (C) Sedimentary structures and colour variation within unit HB1. (D) Wave-rippled silty sand denoting the base of the pit, at 10 m depth. (E) Sedimentary structures within silty sand bed H4. (F) Wave-rippled silty sand beds between 2.6–3.1 m depth. Markings at 0.1 m intervals. Photographs C and D courtesy of Simon Crowhurst.

a silty sand. Three samples were collected for OSL dating. One from the Park Farm Member, at 14.1 m depth, and two from the sandy facies of the Lawns House Farm Member, at 1.9 and 2.6 m depth. However, it should be noted that Bateman *et al*. (2015) are inconsistent regarding the lithostratigraphy of the OSL samples taken from 1.9 and 2.6 m depths. In their Table 1 (p717) it lists the OSL samples as corresponding to the Thorganby Member, but on their Figure 3 (p718) they are annotated as the Lawns House Farm Member. Critically, these samples were collected from sand beds exposed approximately 200 m away from those described in Murton *et al*. (2009) (Figure 1). The age model of Evans *et al*. (2021)

is a revision of Bateman *et al*. (2015), undertaken as part of a wider programme by BRITICE-CHRONO to standardise dating control on the eastern sector of the British-Irish Ice Sheet. The implications of this for the Hemingbrough Formation chronostratigraphy will be discussed later.

The Hemingbrough age models: what is controversial?

Table 1 summarises the sample details and ages determined from the six published OSL ages from Hemingbrough, including the revised ages presented in Evans *et al*. (2021). Two features warrant further scrutiny. First, the two ages from the Lawns House Farm Member sand beds dated by Bateman *et al*. (2015) are not in the correct stratigraphical order, even when the error range is considered. The revised ages of Evans *et al*. (2021) still retain this inconsistency. Second, all three ages determined by Bateman *et al*. (2015) are younger than those determined by Murton *et al*. (2009), regardless of stratigraphical depth. The revised ages presented in Evans *et al*. (2021) still yield younger ages for the Lawns House

Sample details		Dosimetry		Equivalent dose	
Sample	Depth (m)	Water content	Dose rate (Gy/ka)	D_e (Gy)	Age (ka)
HEMA01[1]	1.50 (LHFM)	20	2.4±0.22	54±1.0	21.9±2.0
Shfd11087[2]	1.90 (LHFM)	20 ± 5	2.23±0.06	37.3±0.7	16.8±0.5
Shfd11087[3]	1.90 (LHFM)	23?			19.2±0.5
Shfd11088[2]	2.60 (LHFM)	20 ± 5	2.26±0.07	35.1±0.06	15.5±0.5
Shfd11088[3]	2.60 (LHFM)	23?			18.0±0.6
HEMA02[1]	4.00 (LHFM)	23	2.49±0.23	52.0±1.0	21.0±1.9
HEMA03[1]	4.00 (LHFM)	23	2.17±0.20	52.0±1.0	24.1±2.2
Shfd11093[2]	14.10 (PFM)	25 ± 5	1.04±0.03	22.8±0.5	20.5±0.6
Shfd11093[3]	14.10 (PFM)	23?			22.3±0.7

Table 1. Summary of sample details, dosimetry, equivalent doses and samples ages from Hemingbrough. c [1]Murton *et al*. (2009). [2]Bateman *et al*. (2015). [3]Evans *et al*. (2021). Specific data on revised water content are not listed in Evans *et al*. (2021) but it is assumed either of their values (23% or 27%) applied to samples where "the evidence suggested they had been saturated for most or a substantial part of their burial history" (p735) was used. In addition, Evans *et al*. (2021) applied "wide uncertainties of ± 5% on all water content…to include variations related to porosity and compaction" (p735). The values quoted in Table 1 therefore cite the most likely water content value used.

Farm Member sand beds. But, the age calculated for their lowermost sample, of the Park Farm Member, is near identical to the weighted mean age of 22.2 ± 0.5 of Murton *et al*. (2009) from silty sand beds sampled higher in the stratigraphy.

Bateman *et al*. (2015) do acknowledge that a stratigraphic inconsistency exists between their ages and those previously published by Murton *et al*. (2009). To account for this inconsistency, Bateman *et al*. (2015: 718) observed that "Murton *et al*. (2009) ascribed all sediments to the Park Farm Clay Member, but sampled sandy facies (Murton *et al*., 2009, Figure 3) which appear equivalent to what is ascribed above [in Bateman *et al*., 2015] as the distal facies of the Lawns House Sand Member. That the ages do not agree between their study and this one can be reconciled only if quarrying, in stripping back ~200 m of sediment [the distance between the sampling sites], has now revealed the Lawns House Farm Sand Member and overlying Thorganby Clay Member." In other words, Bateman *et al*. (2015) correlated between sand beds sampled from two sites located just 200 m apart—but at different depths in the stratigraphy—solely on the basis of chronostratigraphy (Figure 3). To put this into context, it would require an abrupt lateral change in sedimentary architecture and exhumation of between 10.1 to 12.6 m of sediment (calculated from their sampling depth of 14.1 m, minus the 4.0 m depth of sand bed H1 or 1.5 m depth of sand bed H4) (Figure 3). How viable is this proposition?

Are there abrupt lateral variations in the Hemingbrough stratigraphy?

The most robust way to test the exhumation hypothesis is to compare the lithostratigraphies and sedimentary properties described in Murton *et al*. (2009) with that of the complete basin-fill. As part of her doctoral research the author had a core drilled to Sherwood Sandstone bedrock at Hemingbrough in 2014, 200 m from the open-face exposure described in Bateman *et al*. (2015) (Figure 1). From this core seven sedimentary units (HBa–HBg) were identified (Figure 4, Table 2). More detailed descriptions of the field and laboratory techniques, sedimentary descriptions and age modelling are given in Murton (2017).

It is apparent that the lithostratigraphy from the Hemingbrough core is consistent with that published by Bateman *et al*. (2015), with both indicating a silty sand bed of notable thickness (0.5–0.6 m) between 13.0 to 14.0 m depths, and interbedded silt and silty sand sediments between 2.0 to 4.9 m depths. Similar interbedded sediments are also recorded between 1.5 to 4.5 m in the 10 m-high field exposure observed by Murton *et al*. (2009).

The field observational data indicate the uppermost interbedded sediments — which include the OSL-dated silty sand beds H1 and H4 — are laterally continuous within the Hemingbrough pit. First, unit HB2 is easily identifiable in field section as the sediments appear darker than the under- or overlying laminated sediments due

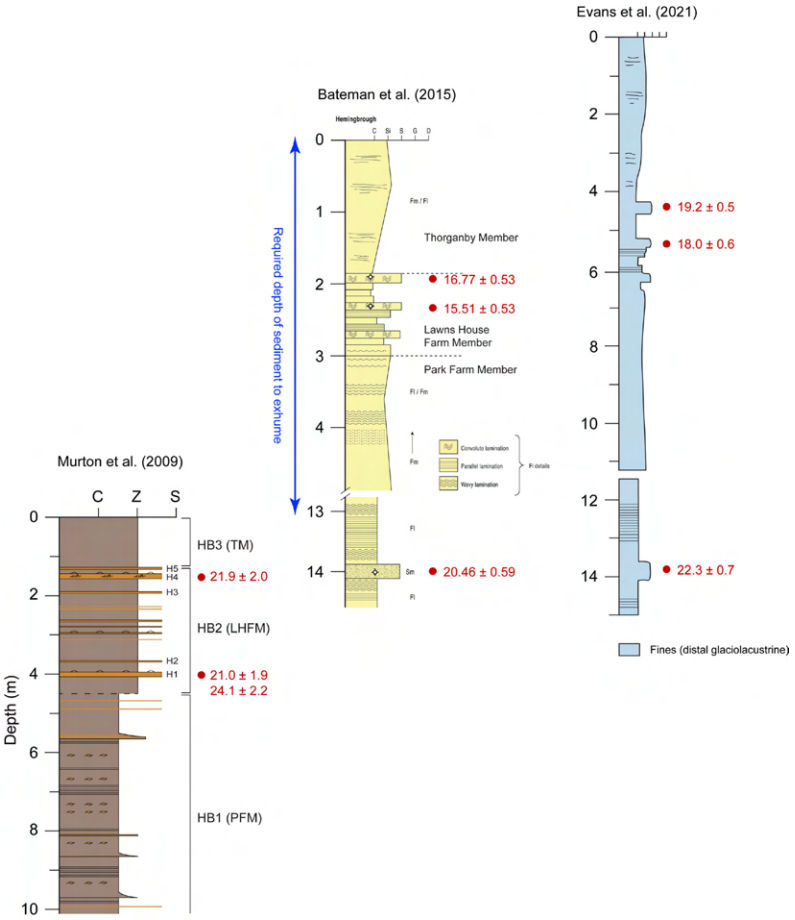

Figure 3. Correlation of dated silty sand sediments at Hemingbrough by BRITICE-CHRONO (Bateman *et al*., 2015; Evans *et al*., 2021) with the original chronostratigraphy of Murton et al. (2009). TM: Thorganby Member; LHM: Lawns House Farm Member and PFM: Park Farm Member. Note Evans *et al*. (2021) have revised both the stratigraphic log and depths of silty sand beds sampled for OSL dating reported originally in Bateman *et al*. (2015).

to continuous water seepage (Figure 5A). Silty sand bed H4 (c.f. Murton *et al*., 2009) in particular forms a marker horizon, visible in both west-east (Figure 5A, 5D) and north-south (Figure 2B, Figure 5B–C. 5E) orientated field sections. It has been observed by the author on every visit to the pit, between 2004 and 2015. It is evident also in Figure 2A (just above the people's heads) of Bateman *et al*. (2015). The silty sand beds become thinner towards the base of unit HB2, but

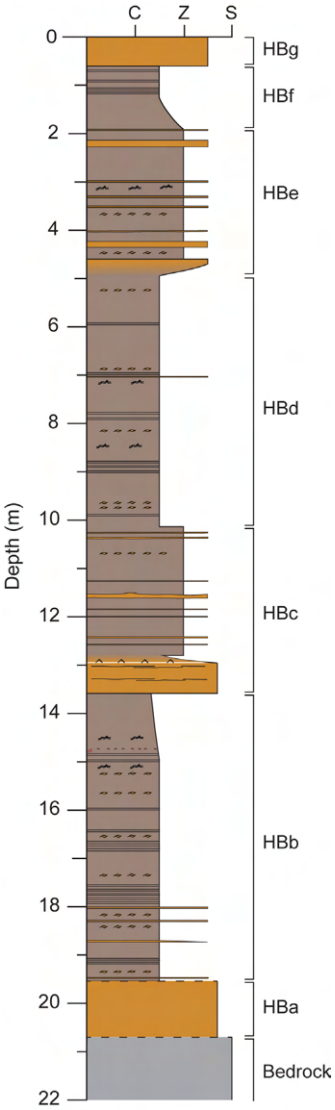

Figure 4. Stratigraphic log for the Hemingbrough core. Legend as for Figure 2.

are still recognisable across the pit (Figure 2A, Figure 5B, 5D–E). Although no field measurements were taken to test whether the depth between silty sand beds H1 and H4 was consistent across the open-face sections between 2004 and 2015, the quarrying owners use the lowermost silty sand beds to identify the contact with the underlying silty clay sediments (used to make bricks) when excavating the pit (Figure 5A). Therefore, both H1 and H4 should be easily identifiable on subsequent visits.

Second, there is no observed change in ground elevation (5 m O.D.) or topography, as evidenced by the pylon in Figure 5E–F. Therefore, any exhumed sediment would have been accommodated by infilling a previously-incised channel, that has been exposed in field section since 2007 (when the author collected the OSL samples, published in Murton *et al*. (2009)). The three-dimensional geometry and sedimentary structures of the interbedded silt and silty sand of lithological unit HB2—that includes beds H1 and H4—is inconsistent with cut and fill processes.

The sedimentological data also negates the exhumation hypothesis. Bateman *et al*. (2015) did not publish any data on sedimentary parameters, so a direct comparison is not possible. However, such data does exist for the Hemingbrough monoliths and core, and as was demonstrated previously, the lithological units are

Lithological unit	Thickness (m)	Sedimentary description
HBg	0.6	Decalcified, organic-rich massive silty sand
HBf	0.9	Mottled, massive to faintly stratified silty clay
HBe	3.4	Massive to faintly stratified silt with silty sand interbeds and laminae
HBd	5.4	Laminated sediments of lighter-coloured silt and darker silty clay couplets interspersed with massive to faintly stratified silty clay
HBc	3.4	Massive to faintly stratified silt with silty sand interbeds and laminae
HBb	5.9	Laminated sediments of lighter-coloured silt and darker silty clay couplets interspersed with massive to faintly stratified silty clay
HBa	1.2	Massive silty sand

Table 2. Summary of the Hemingbrough lithological units and sediments.

laterally extensive across the pit so the sedimentological data should corroborate these observations. This can be exemplified by analysing trends in the magnetic susceptibility data. These data were captured at 2 mm resolution using a Bartington MS2F sensor following the protocol of Dearing (1999). As shown on Figure 6 there are two distinct trends in the magnetic susceptibility records that clearly differentiate lithological units HBc and HBe in the Hemingbrough core. These values progressively increase in the former but progressively decrease in the latter. For lithological unit HB2 in the monoliths the trend is of a progressive decrease in values, consistent with that from unit HBe.

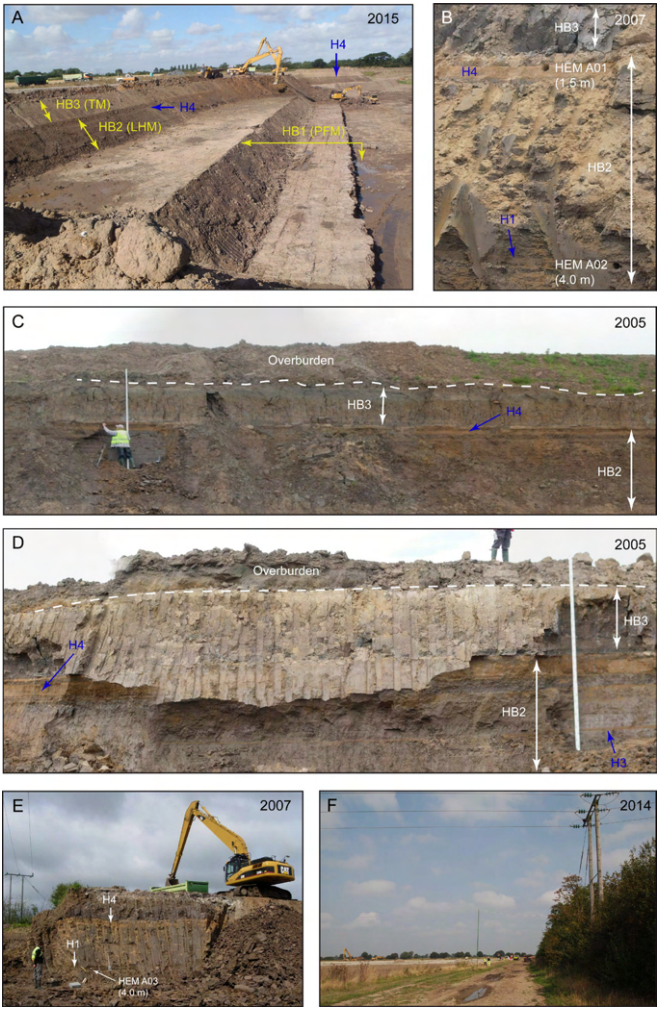

Figure 5. Photographs of the lithostratigraphy at Hemingbrough illustrating (A–E) the lateral extent of key silty sand beds, H4 and H1. H4 is recognisable in the field by its sharp erosive basal contact. HB1: Park Farm Member; HB2: Lawns House Farm Member; HB3: Thorganby Member of the Hemingbrough Formation. Photograph C and D are orientated N–S and W–E respectively. HEMA01, HEMA02, HEMA03 are the OSL sampling sites listed in Table 1. (F) Core sampling site. The pylon in photograph E and F corresponds with the green arrow in Figure 1. Year of visit given in top right-hand corner. Photograph A courtesy of Simon Crowhurst.

In conclusion, the observational and sedimentological evidence is inconsistent with the exhumation hypothesis proposed by Bateman *et al*. (2015) to justify using chronostratigraphy rather than lithostratigraphy to correlate silty sand beds with similar OSL ages. Revising the palaeomoisture content of the silt sands at 14.1 m depth (Evans *et al*., 2021) so that the derived OSL age (22.3 ± 0.7 ka) is consistent with the mean-weighted age (22.2 ± 0.5 ka) of Murton *et al*. (2009) for silty sand beds H1 and H4, situated at least 10.1 m higher in the stratigraphy, still does not reconcile the differences in chronostratigraphy.

An alternative chronstratigraphy for Hemingbrough

A higher-resolution, independent dating control is required against which these conflicting age models can be compared. One technique is palaeomagnetism, in particular relative palaeointensity (RPI). RPI proxies in both lacustrine and marine sediments have been used as a global tool through the correlation of RPI proxies to calibrated reference curves that extend back to 1.5 Ma (e.g. Channell *et al*., 2009). Although calibrated palaeomagnetic secular variation curves currently only exist for the Holocene in northwest Europe (Turner and Thompson, 1978; Snowball *et al*., 2007), RPI records extending into the Devensian glacial Stage do exist for deep-sea cores in the northeast Atlantic Ocean (Channell and Raymo, 2003; Channell *et al*. 2016). Therefore, it might be possible to calibrate a Hemingbrough RPI record with these records, using the OSL ages as chronological tie-points. Core MD04-2822 from the Rockall Trough (Channell *et al*. 2016) (Figure 1) was selected because (a) it is underpinned by a relatively robust age model derived from $\delta^{18}O$ measurements on benthic foraminifera, AMS radiocarbon ages and sea-surface temperatures proxy derived from percentage counts of the planktonic foraminifera *Neogloboquadrina pachyderma (sin)* (Hibbert *et al*., 2010); and (b) both palaeomagnetic measurements were undertaken in the same laboratory, thereby minimising analytical error between the two RPI curves.

U-channel samples were collected from the Hemingbrough core sections and sent for palaeomagnetic analysis at the University of Florida. RPI data were determined from the slope of natural remanent magnetization (NRM) intensity versus (anhysteretic remanent magnetization) ARM intensity, denoted as NRM/ARM. Measurements were at 10 mm intervals. The age models described below were produced using graphic correlation (cf. Prell *et al*., 1986). This is a mathematical technique by which one dataset can be compared against a known reference dataset in order to establish a depth or time series for it, thereby 'fitting' it to the sequence. This technique is widely used in palaeoclimatological reconstructions, for example the LR04 stack (Lisiecki and Raymo, 2005), the PISO-1500 stack (Channell *et al*., 2009), and a global surface ocean $\delta^{18}O$ record (Shakun *et al*., 2015).

Three simple age models (Figure 7A–C) were produced for Hemingbrough. Each model has two chronological tie-points— which, for these reconstructions, are

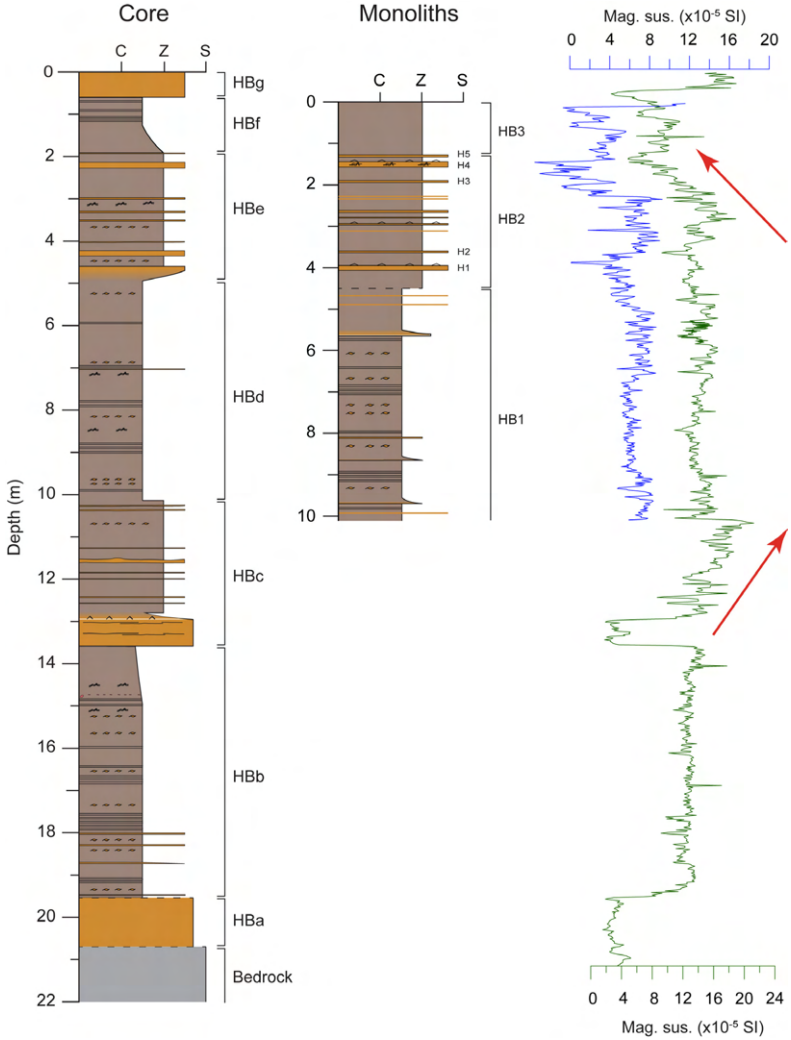

Figure 6. Comparison between the magnetic susceptibility records from the Hemingbrough core and monoliths. Red arrows denote the dominant trend within the interbedded silt and silty sand lithological units.

the OSL ages reported in Table 1—with a chronology established by linearly interpolating between them. The thickest sand bed within unit HBe is at 2.22 m depth (Figure 4), which is interpreted as the lateral extension of silty sand bed H4 observed in field section. The OSL ages reported in Table 1, at 1.5 and 1.9 m

depths, are taken to correspond with bed H4. These depths differ from the core depth because quarrying activities in the Hemingbrough pit most likely removed some of the uppermost sediments whereas the core was drilled on undisturbed ground (Figure 5F) and therefore records the complete lithostratigraphy. Silty sand bed H1 is thinner and less recognisable in the core not least because the number of silty sand beds increases with depth in unit HBe and it could potentially correlate with several of them. For the purpose of these experiments the OSL ages corresponding with 4.0 m depth (the depth of H1 observed in field section) are used. The stratigraphic log from the Hemingbrough core indicates the contact with Lawns House Farm Member and underlying Park Farm Member is at 4.9 m depth. Finally, the basal silty sand bed in unit HBc is interpreted to correspond with the sand bed at 14.1 m depth observed by Bateman *et al*. (2015). Within the core its upper contact is at 13.0 m depth, and this depth is used in the age modelling described below.

Age model 1

This model tests the agreement between the Hemingbrough and MD04-2822 RPI records using the OSL ages from Evans *et al*. (2021), revised from Bateman *et al*. (2015). The chronological tie-points are 19.2 ka (2.22 m) and 22.3 ka (13.00 m); stratigraphic depths are given in parentheses. As shown on Figure 6A the Hemingbrough RPI record is compressed into a very short time span which gives a very limited match to the MD04-2822 RPI record. In this model the age of the contact between the Lawns House Farm Member and the underlying Park Farm Member is 19.9 ka.

Age model 2

Evans *et al*. (2021) also applied Bayesian modelling to their chronological data so as to provide a statistical measure to test the agreement between independently dated sediments, and former ice-sheet limits as determined from the glacial geomorphology and stratigraphy. It is questionable though how independent the chronological data used in the Bayesian modelling are since all the OSL ages previously published by these authors (e.g. Bateman *et al*., 2015, 2018; Evans *et al*., 2018) were revised by adjusting the palaeomoisture content thereby making the sediments older than the ages quoted in the original publications. In the absence of published evidence to the contrary it is presumed the original ages did not provide a statistically significant 'fit' with the interpreted ice limits and were adjusted until they provided a coherent chronology.

The three OSL ages of Murton *et al*. (2009) from Hemingbrough on the other hand are independent, at least within the context of BRITICE-CHRONO, since they were published prior to the initiation of this project. Although these three ages were included in the Bayesian modelling of Evans *et al*. (2021) they were not modified by them. While their modelled output Bayesian median ages (21.9,

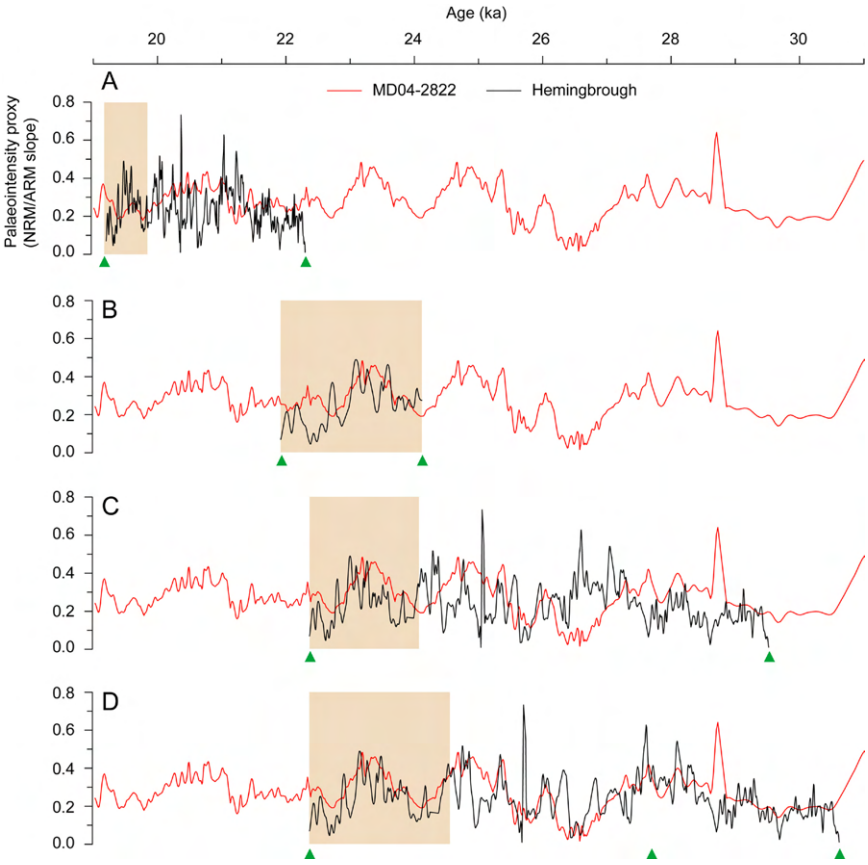

Figure 7. Comparison between RPI records from deep-sea core MD04-2822 and Hemingbrough using OSL ages as chronological tie-points from (A) Evans *et al*. (2021), (B) Murton *et al*. (2009). (C) Mean-weighted OSL age from Murton *et al*. (2009) and the oldest Late Devensian OSL age from North Ferriby of Evans *et al*. (2021). (D) Final calibrated age model. Green triangles denote the chronological tie-points used in each age model. Orange band corresponds with the Lawns House Farm Member.

21.9 and 24.1 ka) remained largely unchanged from the original ages, the Bayesian model identified the oldest OSL age as a clear outlier. Accepting this outcome would imply near-instantaneous deposition of the interbedded silts and silty sands of the Lawns House Farm Member.

To test whether an outlier of 24.1 ka is consistent with the RPI data a second age model applied the OSL ages from Murton *et al*. (2009) as chronological tie-points; namely 21.9 ka (2.22 m) and 24.1 ka (4.00 m). As shown on Figure 7B the trend of the two records is similar though the offset suggests the Hemingbrough sediments are probably slightly older. The age of the contact between the Lawns House Farm and Park Farm members in this reconstruction is >24.1 ka.

Age model 3

This final age model seeks to refine the two RPI calibrations presented previously by applying the mean-weighted age of Murton *et al*. (2009) for the Lawns House Farm Member, and the oldest age reported by Evans *et al*. (2021) for an ice margin in the Humber gap at North Ferriby (Figure 1), as chronological tie-points. These ages are 22.2 ± 0.5 ka (2.22 m) and 29.5 ± 1.7 ka (13.00 m) respectively. Note that the latter age has been significantly revised from the original age of 22.5 ± 1.6 ka reported by Bateman *et al*. (2018).

As shown on Figure 7C the trends of the Hemingbrough and MD04-2822 RPI records are in good agreement though there are offsets. The calibration can be refined further (Figure 7D) by adding a secondary tie-point and increasing the age of the lowermost chronological tie-point to 30.6 ka, which is within error of the age of Evans *et al*. (2021). The age of the contact between the Lawns House Farm and Park Farm members in this reconstruction is 24.5 ka. This age model is consistent with that originally proposed by Murton (2017).

Conclusion

Conflicting chronologies determined from OSL dating of silty sand beds sampled from the uppermost 14 m of sediments at Hemingbrough have been tested by comparing a RPI record from this site with a calibrated RPI record from deep-sea core MD04-2822 in the adjacent Rockall Trough. The 'best-fit' correlation indicates that the Hemingbrough sediments are older than the chronology proposed by BRITICE-CHRONO, with deposition occurring throughout the Late Devensian rather than just during the Last Glacial Maximum. This has critical implications for the palaeoenvironmental reconstructions presented in Evans *et al*. (2021), which will be assessed in detail elsewhere (Murton, in prep).

Acknowledgements

Plasmor are thanked for continued access to the Hemingbrough pit, with Julian Murton and Jim Rose assisting with monolith sampling at this site. Rob Cooke at SOCOTEC UK, and GeoSonic are thanked for core drilling and field support. Jim Channell and Kianian Huang, University of Florida, and David Hodell and the Godwin Laboratory for Palaeoclimate Research, University of Cambridge kindly provided technical support. Comments by Gordon Bromley are much appreciated.

References

Bateman, M.D., Evans, D.J.A., Buckland, P.C., Connell, E.R., Friend, R.J., Hartmann, D., Moxon, H., Fairburn, W.A., Panagiotakopulu, E., Ashurst, R.A. (2015). Last glacial dynamics of the Vale of York and North Sea lobes of the British and Irish Ice Sheet. *Proceedings of the Geologists' Association*, 126, 712–730.

Bateman, M.D., Evans, D.J.A., Roberts, D.H., Medialdea, A., Ely, J., Clark, C.D. (2018). The timing and consequences of the blockage of the Humber Gap by the last British-Irish Ice Sheet. *Boreas*, 47, 41–61.

Channell, J.E.T., Raymo, M.E., (2003). *Paleomagnetic record at ODP Site 980 (Feni Drift, Rockall) for the past 1.2 Myrs*. Geochemistry, Geophysics, Geosystems, 4, 1033, doi:1010.1029/2002GC000440.

Channell, J.E.T., Xuan, C., Hodell, D.A. (2009). Stacking paleointensity and oxygen isotope data for the last 1.5 Myr (PISO-1500). *Earth and Planetary Science Letters*, 283, 14–23.

Channell, J.E.T., Harrison, R.J., Lascu, I., McCave, I.N., Hibbert, F.D., Austin, W.E.N. (2016). *Magnetic record of deglaciation using FORC-PCA, sortable-silt grain size, and magnetic excursion at 26 ka, from the Rockall Trough (NE Atlantic)*. Geochemistry, Geophysics, Geosystems ,17, doi:10.1002/2016GC006300.

Dearing, J., (1986). *Magnetic susceptibility*. In: Walden, J., Oldfield, F., Smith, J. (Eds.) Environmental Magnetism: a practical guide. Technical Guide 6, pp. 35-62. Quaternary Research Association, London.

Evans, D.J.A., Roberts, D.H., Bateman, M.D., Clark, C.D., Medialdea, A., Callard, L., Grimoldi, E., Chiverrell, R.C., Ely, J., Dove, D., Ó Cofaigh, C., Saher, M., Bradwell, T., Moreton, S.G., Fabel, D., Bradley, S.L., (2021). Retreat dynamics of the eastern sector of the British–Irish Ice Sheet during the last glaciation. *Journal of Quaternary Science*, 36, 723-751.

Ford, J.R., Cooper, A.H., Price, S.J., Gibson, A.D., Pharoah, T.C., Kessler, H. (2008). Geology of the Selby district - a brief explanation of the geological map 1:50 000 Sheet 71 Selby (England and Wales). British Geological Survey, Nottingham.

Gaunt, G.D. (1994). *Geology of the Country around Goole, Doncaster and the Isle of Axholme*. Memoir for one-inch sheets 79 and 88 (England and Wales). HMSO, London.

Gaunt, G.D., Fletcher, T.P., Wood, C.J. (1992). *Geology of the country around Kingston upon Hull and Brigg*. Memoir for 1:50 000 geological sheets 80 and 89 (England and Wales). HMSO, London.

Hibbert, F.D., Austin, W.E.N., Leng, M.J., Gatliff, R.W., (2010). British Ice Sheet dynamics inferred from North Atlantic ice-rafted debris records spanning the last 175 000 years. *Journal of Quaternary Science*, 25, 461-482.

Lisiecki, L.E., Raymo, M.E. (2005). A Pliocene-Pleistocene stack of 57 globally distributed benthic δ18O records. *Paleoceanography*, 20, PA1003, doi:1010.1029/2004PA001071.

Murton D.K. (2017). *Late Pleistocene palaeoenvironmental change in the Vale of York and Humber gap*. Unpublished PhD thesis, University of Cambridge. 286pp.

Murton, D.K., Pawley, S.M., Murton, J.B. (2009). Sedimentology and luminescence ages of Glacial Lake Humber deposits in the central Vale of York. *Proceedings of the Geologists' Association*, 120, 209–222.

Prell, W.L., Imbrie, J., Martinson D.G., Morley J.J., Pisias N.G., Shackleton N.J., Streeter H.F. 1986. Graphic correlation of oxygen isotope stratigraphy application to the late Quaternary. *Paleoceanography*, 1, 137–162.

Shakun, J.D., Lea, D.W., Lisiecki, L.E., Raymo, M.E., (2015). An 800-kyr record of global surface ocean δ18O and implications for ice volume-temperature coupling. *Earth and Planetary Science Letters*, 426, 58–68.

Snowball, I., Zillén, L., Ojala, A., Saarinen, T., Sandgren, P. (2007). FENNOSTACK and FENNORPIS: Varve dated Holocene palaeomagnetic secular variation and relative palaeointensity stacks for Fennoscandia. *Earth and Planetary Science Letters*, 255, 106–116.

Thomas, G.S.P., (1999). Northern England In: Bowen, D.Q. (Ed.) A revised correlation of Quaternary deposits in the British Isles, pp. 91-98. Geological Society Special Report no 23, London.

Turner, G.M., Thompson, R. (1981). Lake sediment record of the geomagnetic secular variation in Britain during Holocene times. *Geophysical Journal of the Royal Astronomical Society*, 65, 703–725.

THE CLOGHMORE* ERRATIC (MOUNTAINS OF MOURNE, NORTHERN IRELAND) IS UNLIKELY TO BE A VISITOR FROM SCOTLAND

Peter Wilson

School of Geography and Environmental Science, Ulster University, Coleraine, Co. Londonderry BT52 1SA, Northern Ireland
p.wilson@ulster.ac.uk

Introduction

In the Introductions of two recent Quaternary field guides to the Mountains of Mourne, Northern Ireland, the caption that accompanies an image of the Cloghmore erratic boulder states that "It is thought to have been transported by Scottish ice and originated from the Firth of the Clyde". The image is credited to Conor Graham but the source of the caption is not clear (Roberson, 2016, 2019). However, no evidence in support of this assertion of Scottish provenance was provided in the field guides. If the boulder had been transported and deposited by ice emanating from Scotland, presumably during the late Devensian/Midlandian glaciation (~32-15 ka), it would have implications for the direction of ice flow from the northern sector of the Irish Sea Basin. The ice would have had to have moved either southwest across the Mountains of Mourne or southwest across the Mourne Plain, to the south of the mountains, and then west into the Carlingford trough. The purpose of this note is to argue that the boulder and adjacent erratics are likely to be of more local (Irish) derivation, rather than from Scotland, and to highlight concerns about using and apparently accepting information without question.

Location and setting

Cloghmore is a large (~4.5x3.9x2.4 m) granite boulder perched on Silurian metasedimentary bedrock at 285 m OD (Grid Reference J 192 173) on the southern margin of the Mountains of Mourne (Figure 1). It stands on a prominent knoll on the undulating west-to-northwest ridge of Slievemeen (472 m OD) above the place where the ridge falls steeply towards the town of Rostrevor and the northern shores of Carlingford Lough (Figure 2). Adjacent to Cloghmore are numerous smaller granite boulders.

Source of Cloghmore

Although Cloghmore and neighbouring granite boulders are clearly ice-transported, no previous mainstream reports on the glacial history of the Mournes link them to Scottish ice. Charlesworth (1939) regarded Cloghmore as part of a moraine of large granite boulders associated with his Carlingford Re-advance (i.e. ice

Figure 1. The Cloghmore granite erratic resting on Silurian metasedimentary bedrock. Smaller boulders in front of and to the left of the person are also granite.

flow from north central Ireland towards the Irish Sea). Subsequently, McCabe *et al*. (1999), Greenwood and Clark (2009a, b) and Smith and Knight (2011) have identified a similar ice-flow pattern based on a variety of indicators, but they also recognise that early in the last glacial cycle there was an incursion of ice from Scotland across the Mourne region, and erratics from Scotland are known from various places along the north and east coasts of Ireland (Dwerryhouse, 1923; Charlesworth, 1939).

Therefore Cloghmore could have been sourced in and carried from Scotland during this early phase of the Late Devensian/Midlandian glaciation. However, during and subsequent to the local Last Glacial Maximum (lLGM; ~27-25 ka) the Carlingford area was dominated by ice flows from dispersal centres in north central Ireland and the Mourne Mountains north of Rostrevor. These flows crossed granitic rocks of the Slieve Gullion Complex, Newry Complex, and the Mourne Complex (Figure 2).

Cloghmore lies just 2.5 km from the southern margin of the Mourne granite, and that granite mass extends 19 km to the northeast. Granite boulders are also abundant along the valley of the Kilbroney River and its east side bounding ridge from Slievedermot to Slievemeen (Figure 2). They are present at the summit of Slievemartin but are incorporated in an archaeological structure and therefore

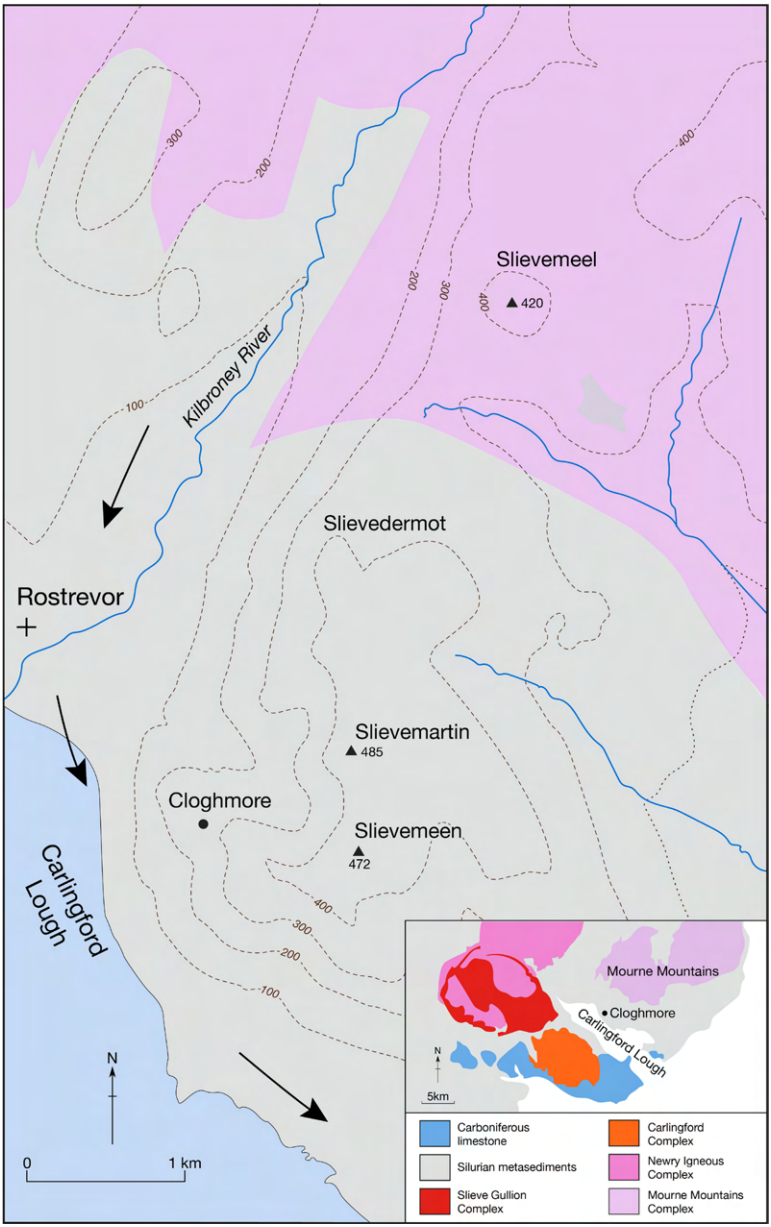

Figure 2. Bedrock geology based on Institute of Geological Sciences (1978), topography, ice flow directions (arrows) and location of the Cloghmore erratic. Inset shows bedrock types around Carlingford Lough.

may have been moved to that location by humans. However, given the proximity of these erratics to the granite outcrop and their down-valley distribution from it, it seems only reasonable, in the absence of comparative mineralogical data, that Quaternary scientists should apply the principle of Occam's razor to account for their presence – i.e. the simplest explanation is that they probably derive from the Mourne granite outcrop rather than being far-travelled visitors from Scotland.

Wider concerns

Although the origin of Cloghmore is of only minor significance in the greater scheme of lLGM ice flow, it concerns me that the Scottish connection is perpetuated in some literature. I do not know where and when a Scottish connection was first suggested for Cloghmore or on what basis, but an Internet search for 'Cloghmore glacial erratic' throws up several sites that repeat the claim. Some of these refer to an article entitled Drumlin Country, by John McCullagh, published in 2004 in the *Newry Journal*, in which it is claimed that Cloghmore was "carried from an island in Strathclyde bay".

What surprises me is that this information has been repeated in recent field guides without being examined and/or challenged. If we, as Quaternary scientists, fail to query such statements when more plausible alternatives exist, we do our science and our students a serious injustice.

*Alternative spelling: Cloughmore.

References

Charlesworth, J.K. (1939). Some observations on the glaciation of north-east Ireland. *Proceedings of the Royal Irish Academy,* 45B, 255-295.

Dwerryhouse, A.R. (1923). The glaciation of north-eastern Ireland. *Quarterly Journal of the Geological Society*, 79, 352-422.

Greenwood, S.L. and Clark, C.D. (2009a). Reconstructing the last Irish Ice Sheet 1: changing flow geometries and ice flow dynamics deciphered from the glacial landform record. *Quaternary Science Reviews,* 28, 3085-3100.

Greenwood, S.L. and Clark, C.D. (2009b). Reconstructing the last Irish Ice Sheet 2: a geomorphologically-driven model of ice sheet growth, retreat and dynamics. *Quaternary Science Reviews,* 28, 3101-3123.

McCabe, A.M., Knight, J. and McCarron, S.G. (1999). Ice-flow stages and glacial bedforms in north central Ireland: a record of rapid environmental change during the last glacial termination. *Journal of the Geological Society, London,* 156, 63-72.

Institute of Geological Sciences. (1978). *Mourne Mountains*. Northern Ireland

Special Sheet, Solid Edition. Institute of Geological Sciences/Geological Survey of Northern Ireland.

Roberson, S. (2016). Introduction to the 2016 field meeting. In: Roberson, S., Barr, I. and Cooper, M. (eds). *The Quaternary glaciation of the Mourne Mountains: Field Guide*. Quaternary Research Association, London, 1-6.

Roberson, S. (2019). Introduction. In: Roberson, S. (ed.). *The glaciation of the Mourne Mountains*. XX INQUA Congress Field Guide, Irish Quaternary Association, Dublin, 1-6.

Smith, M.J. and Knight, J. (2011). Palaeoglaciology of the last Irish ice sheet reconstructed from striae evidence. *Quaternary Science Reviews,* 30, 147-160.

A ROAD SECTION THROUGH THE UPPER PLEISTOCENE COASTAL CLIFFS AT ACCRA BEACH, BARBADOS

William Fairburn

Introduction

The island of Barbados, which is about 34 km long and 24 km at its widest, lies along the eastern boundary of the Caribbean Sea with the Atlantic Ocean and to the east of the volcanic island arc system of the Lesser Antilles that extends from north of Antigua to south of St Lucia (Fig 1a). This group of islands are also referred to as the Leeward Islands (to the north) and the Windward Islands (to the south).

The purpose of this article is to describe an easily accessible road verge section leading to the top of the coastal cliff at the southern end of Accra Beach and place it in the geological and chronological framework of Barbados.

Barbados – geology and chronology

Geologically, Barbados lies on the Caribbean side of a subduction zone where the Caribbean Plate is underridden by the South American Plate (Westbrook, *et al*., 1973). According to Donovan (2005), the island is composed entirely of a sedimentary sequence apart from some volcanic ash bands. Some eighty-five per cent of this sequence are Pleistocene reef limestones while the remainder are Tertiary sedimentary rocks of marine origin that outcrop in the north-east of the island in an area referred to as the Scotland District (Figure 1b).

The reef limestones form a rising staircase morphology of terraces or tracts, for the island, resulting from a combination of high sea stands and tectonic uplift (Bender *et al*., 1979). Up to ten of these reef tracts were recognized, many of which were illustrated by Donovan (2005, Figure 9). The most important tracts i.e. the Lower, Middle and Upper Coral Rocks are outlined on the simplified geological map of Barbados (Figure 1b) Uranium-series dating of corals, still in their original aragonite state, from these major tracts gave ages of 120 ka or 125 ka for the Lower Coral Rock (Teh-Lung, 1968; Matthews, 1973; Bender *et al*., 1979 and Humphry and Matthews, 1986), 350 ka for the Middle Coral Rock (Bender *et al*., 1973) and 480 ka and 500 ka for the Upper Coral Rock (Bender *et al*., 1973). Older ages dating back to 650 ka have been reported by Bender *et al*. (1973). Two younger tracts in the coastal cliffs below the Lower Coral Rock gave ages of 80-82 ka (Teh-Lung, 1968; Matthews, 1973; Bender *et al*., 1979 and Humphrey and Matthews, 1986) and 105 ka (Teh-Lung, 1968; Matthews, 1973; and Bender *et al*., 1979).

Donovan (2005) has estimated that the uplift of the coral reefs on Barbados is in the region of 300 mm per 1000 years; an uplift he considered to have persisted for 700 ka. This uplift calculation is based on the elevation difference (presumably *c* 13 m) between the 82 ka tract and the 125 ka tract at South Point (Figure 1b). Broecker *et al*., (1968) had earlier considered that a uniform rate of uplift was 'fast enough to separate in elevation, coral-reef tracts formed at high stands of the sea'. Compared with other authors (referred to above) they recognized distinct stands at 82 ka, 103 ka and 122 ka. Similar references to an association of Late Pleistocene high stands with coral reef tract formation has been made by Matthews (1973) and Bender *et al*., (1979). Matthews (1973) has suggested that the Lower Coral Rock tract, dated to 125 ka B.P. could be equated to MIS 5 and therefore possibly equivalent in age to the Sewerby raised beach for which Bateman and Catt (1996) gave a minimum luminescence age of 120.8 ka ± 11.8 ka and dated to oxygen isotope stage (OIS) 5e. Bender *et al*. (1979) have also suggested that younger tracts, which they date 82 ka and 105 ka B.P., could record interstadial periods. The above data is indicative of using Barbados coral tracts as a dipstick for the Late Pleistocene high sea level stands.

The Accra Beach Section

This section, readily accessible at the southern end of the Accra Beach at Rockley, forms a narrow ledge, up to about 0.5m high (Figure 1d), that extends for about 20 m on the southern side of an inland road that leads to the top of the 4 m high coastal cliffs (Figure 1c) overlooking Accra Beach. Although this section was not referenced by Donovan (2005), the cliff section it exposes is most likely equivalent to that in the coastal cliffs at South Point dated to the 82 ka tract by Donovan (2005, see Figure 9).

At South Point, the modern-day sea cliffs, dated to 82 ka (Humphrey and Matthews, 1986), are formed by raised reef limestones composed of the colonial coral Acropora cervicornis. A.cervicornis belongs to an order of scleractinian hexacorals that build both solitary and colonial forms that range from the present day back to the Middle Triassic (Shrock and Twenhofel, 1953). At Accra Beach the colonial corals have not been identified.

References

Bateman, M.D., Catt, J.A. (1996). An absolute chronology for the raised beach and associated deposits at Sewerby, East Yorkshire, England. *Journal of Quaternary Science,* 11, 389-395.

Bender, M.L., Taylor. P.T., Matthews, R.K. (1973) Helium-uranium dating of corals

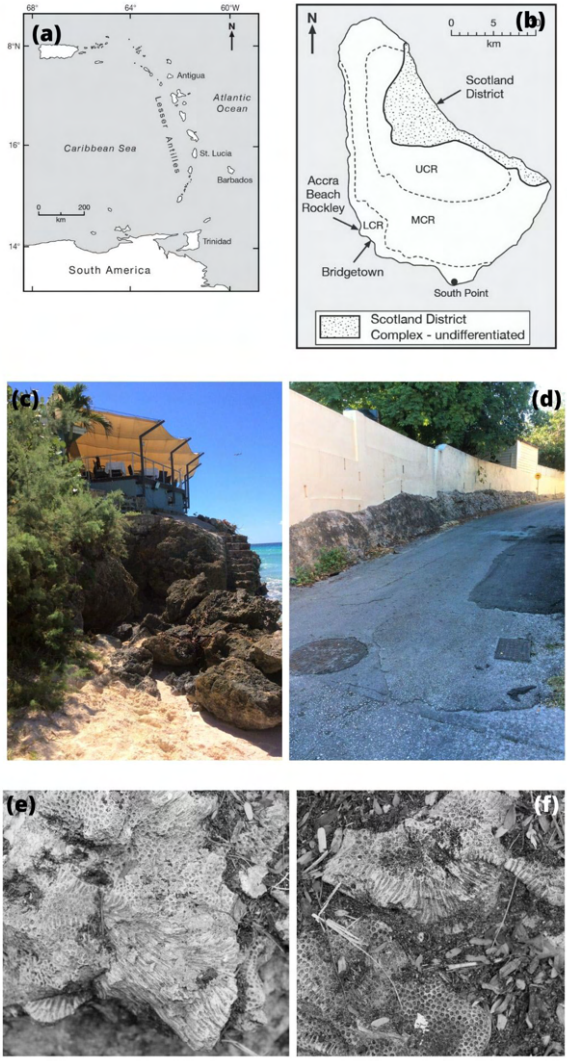

Figure 1. Barbados maps with photographs of the coastal cliffs south of Accra Beach. (a) The location of Barbados between the Atlantic Ocean and the Caribbean Sea. (b) Simplified geological map of Barbados: LCR/MCR/UCR = Lower/ Middle and Upper Coral Rocks after Donovan (2005). (c) A raised coral reef forming the coastal cliffs at the Southern end of Accra Beach – section *c*. 3m (d) Road section from the top of the coastal cliffs – the white wall is approximately 2.0m high. (e) and (f) photographs of the colonial reef forming corals – the small leaves are about 2.5cm. Photographs from W. Fairburn ('c' and 'd') and T. Keena ('e' and 'f').

from Middle Pleistocene Barbados reef tracts. *Quaternary Research,* 3, 142-146.

Bender, M.L., Fairbanks, R.G., Taylor, F.W., Matthews, R.K., Goddard, J.G., Broecker, W.S. (1979). Uranium series dating of the Pleistocene reef tracts of Barbados. *Geological Society of American Bulletin,* 90, 577-594.

Broecker, W.S., Thurber, D.L., Goddard, J., Teh-Lung, Ku, Matthews, R.K., Mesolella, K.J. (1968). Milankovitch hypothesis supported by precise dating of coral reefs and deep-sea sediments. *Science,* 159, 297-300.

Donovan, S.K. (2005). The geology of Barbados: a field guide. *Caribbean Journal of Earth Science,* 38, 21-33.

Humphrey, J.D., Matthews, R.K. (1986). The Pleistocene coral cap of Barbados. In Anon (ed.), *11th Caribbean Geological Congress Barbados – 1986. Field Guide, Barbados, July 1986*. Government Printing Department, Bridgetown, Barbados, pp.85-105.

Matthews, R.K. (1973). Relative elevation of Late Pleistocene high sea level stands: Barbados uplift rates and their implications. *Quaternary Research,* 3, 147-153.

Shrock, R.S., Twenhofel, W.H. (1953). *Principles of invertebrate palaeontology* – second edition. McGraw-Hill Book Company, Inc., New York, 816pp.

Teh-Lung Ku. (1968). Protactinium method of dating coral from Barbados Island. *Journal of Geophysical Research,* 73, 1896 - 1977.

Westbrook, G.K., Bott, M.H.P., Peacock, J.H. (1973). Lesser Antilles subduction zone in the vicinity of Barbados. *Nature,* 244,118-120.

William A. Fairburn
Apartment 101, Core 3,
Leetham House
Palmer Street
York
YO1 7PD
Williamfairburn001@yahoo.com

POTENTIAL OF SWISSTOPO AND SWISS GEOLOGICAL SURVEY WEBSITES FOR QUATERNARY RESEARCHERS

David Nowell

During the last few years, the Federal Office of Topography in Switzerland has been developing an outstandingly diverse and rich multilingual source of online geodata, historic photographs and digital topographic images. While you have to pay for some data sets, most of this is freely available. Bespoke pdf extracts can be download using the print bar with a clear series of options. This flexible data viewer allows users to choose from a wide range of layers, starting with simple cartographic extracts, to self-generated mixes incorporating other spatial information (Figure 1). Files can be generated at a wide range of scales, complete with compass north and scale bar. It also features published and out of print 25k geological maps, national geological vector datasets, plus related thematic maps in additional layers. These can also be downloaded via a separate website as zip folders containing TIF files from which it is easy to make extracts, plus pdf copies of memoirs. Considering this wealth of material, this article aims to provide a broad overview with illustrated examples, rather than providing a detailed introduction to the Quaternary geology of Switzerland.

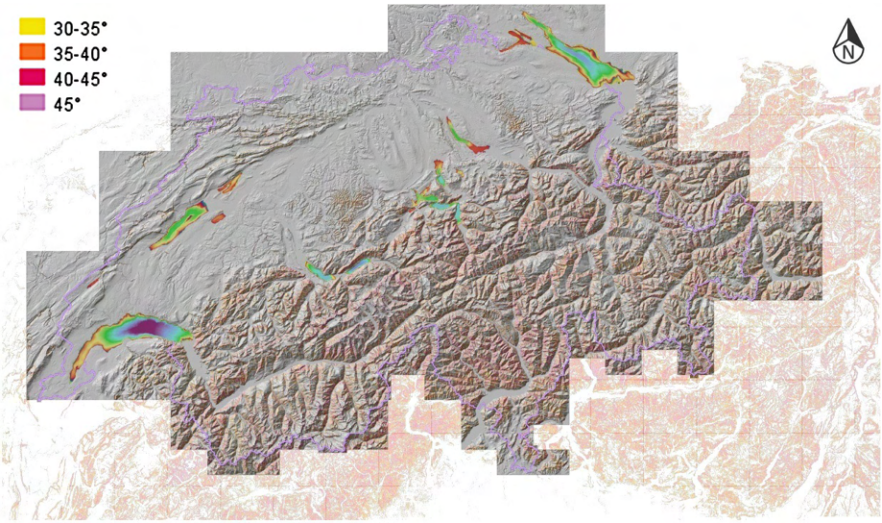

Figure 1. A mixed output map of Switzerland extending into adjacent countries, with DHM25 hillshade derived from digital elevation model as the most dominant half filtered transparency layer, combined with false colour bathymetric hillshade for selected lakes and steep slopes over 30 degrees subdivided into bands with over 45 degrees in purple including data for France, Italy, Austria and Liechtenstein.

Depending how you enter the main viewer from the options listed on the **Freely Available Online Tools** webpage, you will start off with a range of topics on the left-hand side of the screen, with the one already on display having a tick in its box. Thus, it is possible to toggle between layers simply by clicking boxes on and off. Straight above Maps displayed, layers within pre-set themes can be added via the Change topic bar. Also, the search option right at the top of the screen can be used to find extra layers. The i next to each topic provides an information button with a quick summary about each layer. These brief technical descriptions can be translated between German, French, Italian, English and Romansh, simply by changing the language option in the top right-hand corner.

Within Maps displayed, clicking the black circle on the right-hand side of a topic, opens up a transparency slider, and up and down arrows to change their relative order. Depending on which layers are uppermost they will take precedence when the transparency slider is used to allow other layers to show through. This example shows variations in the quality of geological surveying between neighbouring sheets in the Geological Atlas of Switzerland (sequential numbering starting with the first sheet published in 1930), plus blended GeoCover vector data (Fig 2), south of Schaffhausen on the Rhine and border with Germany. These data files for each sheet in the national 25k topographic series can also be freely downloaded as zipped folders via a separate link.

Alpine Rhône delta and offshore channels

An example of what is easily possibly comes from focusing on the Alpine Rhône delta where it flows into Lake Geneva (Lac Leman) to produce this composite image (Fig 3). The drained alluvial plain extends out towards the lake, including Le Petite Camargue holiday village, sited between Canel Stockalper and the main river. For the last few km, the course of the Vieux Rhône can still be picked up as a small stream between the modern Rhône and the Grand Canel to its east (Sastre *et al*. 2010). In many ways this former marshland can be considered a miniature version of the Camargue delta, with its river channels flowing into the Mediterranean. Though the equivalents of the channels seen disappearing into the lake's depths, are buried by sediments filling the Gulf of Lions, can be picked up in seismic images (Bache *et al*. 2009). Also, changes in denudation rates and sediment supply over the Pliocene and Quaternary have been studied in detail (Molliex *et al* 2016), alongside sediment yields within the Provence Basin (Leroux *et al*. 2017). In other places, similar more deeply eroded canyons have developed along the edge of the Mediterranean continental shelf, with much greater erosive potential along bathymetric profiles down to depths of several km (Lofi 2018; Nowell 2021b), compared to Lake Geneva which reaches a maximum depth of 310 m, 62 m above mean sea level.

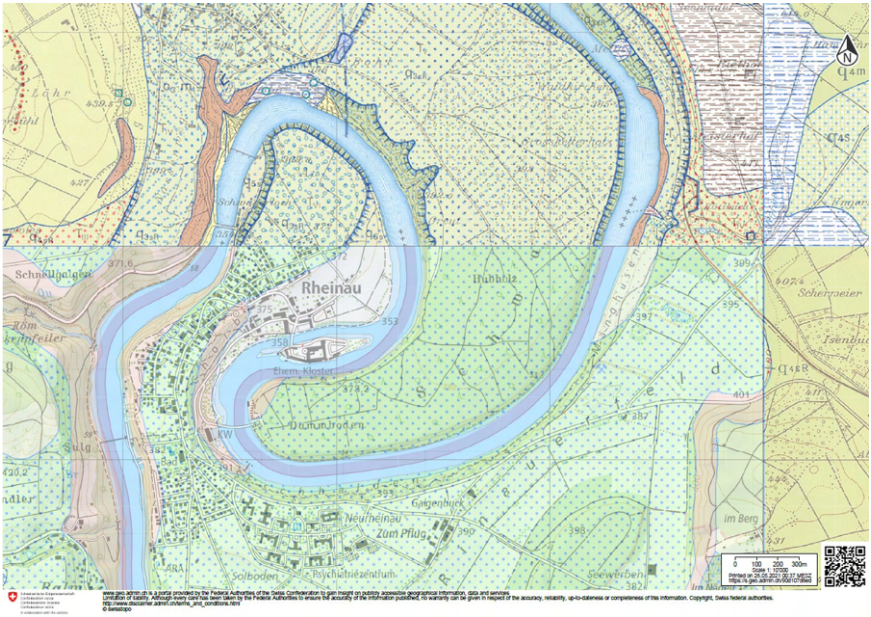

Figure 2. Example different generations of 1:25,000 geological mapping around Rheinau: Northern portion, Sheet 74 Neunkirch (1031) published in 1981; NE extract, Sheet 38 Diessenhofen (1032) 1961; SE extract, Sheet 52 Andelfingen (1052) 1967; Southern portion, Eglisau (1051) consisting of GeoCover 2020 edition and 25k topographic mapping. This mainly shows extent of river terraces, with glacial moraines and tills on higher ground, plus peat bogs marked with horizontal dots and dashes near NE corner, with Miocene bedrock in darker browns. Copyright © swisstopo, All rights reserved

However, early investigations of this miniature delta were highly influential in studies of other river systems (Girardclos *et al*. 2012). Since the 1960s it has become increasingly clear turbidity currents play a significant factor in the evolution of channel systems flowing down onto floor of Lake Geneva (Fig 3). After 1982, these studies since include exploration with submersibles the main channel that about a km offshore turns westwards and flows roughly parallel to the south shore (Girardclos *et al*. 2012).

Extent of superficial deposits

Another image generated with this system, shows the extent and depth of superficial deposits across NE Switzerland combined with current rates of uplift, simply to merge two data sets (Fig 4). Though they are probably unrelated, the pattern of changes in elevation will be a complex combination of post glacial uplift (Nowell

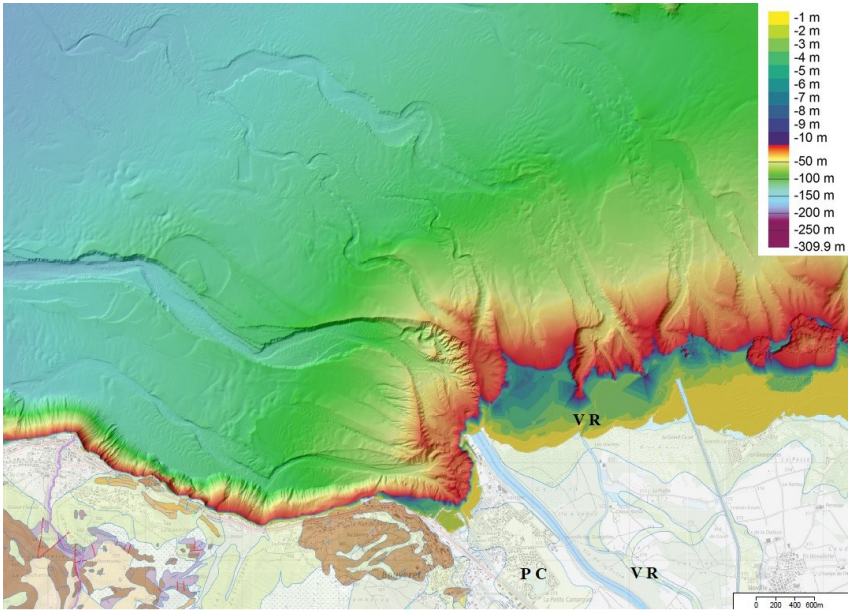

Figure 3. The southern shores of Lake Geneva and Alpine Rhône delta showing sinuous offshore channels picked out by false colour bathymetry. Combined with GeoCover 2020 edition, based on 25k geological sheet 47 Montreux (1264), mixed with modern topographic mapping to provide an up to date base map. P C = Le Petite Camargue holiday village between main river channel and Canel Stockalper to its west; V R = Vieux Rhône with Grand Canel further east. Copyright © swisstopo, All rights reserved

et al. 2006, appendix 1) and plate tectonic forces. However, the thickness data reveals a significant number of buried valleys with the current interpretation of borehole, seismic and other geophysical data. This is based on modelling with some simplification used to plot these variations in thickness. In many places there is little difference with earlier studies (Jordon 2010; Preusser *et al*. 2010; Cohen *et al*. 2017), but about 14 km south of Konstanz, a buried valley is clearly shown linking just south of Amriswil with Sulgen to the southern outskirts of Weinfelden going east to west. This can be toggled with a bedrock elevation model of the surface below unconsolidated deposits. In places this underlying morphology is surprisingly sharp, showing the relief within buried valleys formed by water flowing at pressure under the base of ice sheets, often eroding localised weaknesses within the bedrock.

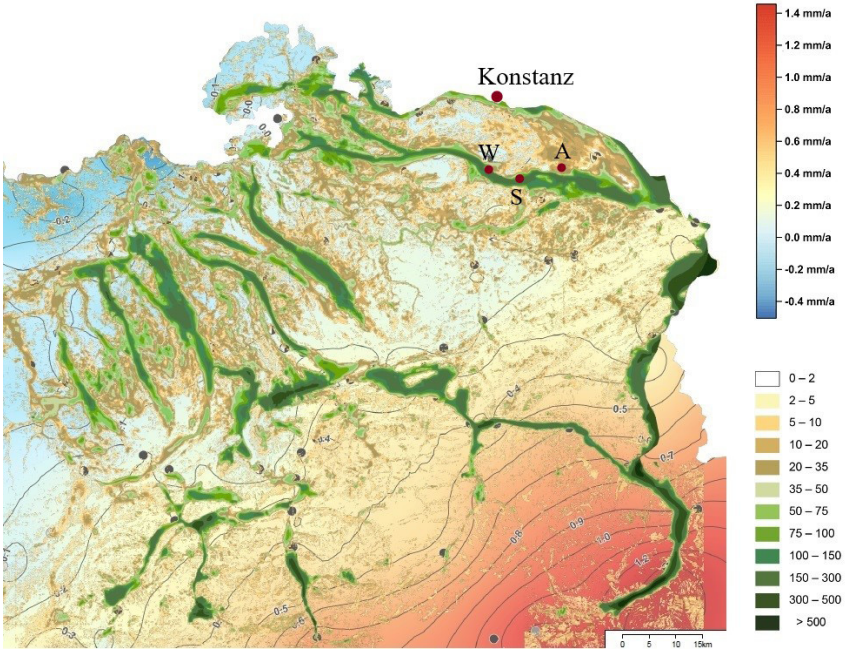

Figure 4. Thickness of superficial deposits, starting with yellow, orange and brown tints, before green tones indicate accumulations greater than 35 m right down to over 500 m deep around Sargans and Diepoldsaur along Alpine Rhine valley, combined with changes in elevation relative to Aarburg - an arbitrary reference point. This shows through in areas with near surface bedrock, contoured in tenths of a mm a year, below and the same as Aarburg in blue tones, and faster rates of uplift in yellow, orange and red tones, including Liechtenstein. Circles denote different types of fundamental bench marks. W = Weinfelden; S = Sulgen; A = Amriswil. Copyright © swisstopo, All rights reserved

Geological map downloads

Supplementing this are the geology geodata webpages, with digital downloads plus published and out of print geological and thematic maps at all scales. In most cases this includes accompanying memoirs, which also contain plates with cross sections, and possibly extra diagrams and maps tacked right on the end. Given they are printed separately these should be provided as TIF copies, alongside the 25k geological maps and marginalia in this flexible format. These are in two different versions, because the geodetic reference frame, was updated from LV03, to LV95 which became the official system in 2016. Locations have been translated by up to 1·6 m as a result, and heights slightly adjusted due to the treatment of vertical movements and gravity reductions (Geodesy 2016). This is why the zip folders containing these geological map downloads are well over 100 Mb. Swisstopo

have even calculated the volumetric centre of Switzerland, grid reference 674,533 167,450 and 902 m in altitude, below the ~3,300 m flanks of Eggstock. Thus, Switzerland covers 41,284·3 km^2 and has a volume of 53,958·1 km^3.

The latest 25k editions show superficial deposits in much more detail than before, supplemented by plates with beautifully drawn cross sections illustrating vertical and lateral changes between meticulously grid referenced points. These are similar to the more generalised schematic cross sections on the margins of British Geological Survey – BGS 50k maps, before publication was halted (Nowell 2014a). Also, on the Bureau de Recherches Géologiques et Minières - BRGM InfoTerre viewer, parts of France look decidedly dated given some 50k sheets were published over 60 years ago, and compare poorly with adjacent 21st century geological maps and modern Swiss coverage (Nowell 2020). Boreholes reaching the bedrock are depicted as circles filled with that colour, alongside its depth beneath the overlying superficial deposits, while solid blue circles are boreholes which did not reach this surface with their depth.

Map extracts and cross sections

This extract from Sissach – Rheinfelden (1068-1048) an extended sheet straddling the High Rhine (Pfirter *et al*. 2019), includes an area where Lower Pleistocene gravels are masked by Löss deposits (Fig 5a), revealed by this cross section (Fig5b). Near Möhliner, a complex sequence of Middle Pleistocene glaciofluvial gravels, blanketed by Löss and weathered loam and slope deposits, mainly consists of Alpine, along with some Black Forest derived material. This cross section shows glaciotectonic deformation with faults and thrusting seen in the Bünten gravel pit (Fig 5c). Just west of this line at Hübel, Löss deposits were sampled for thermoluminescence dating, and the underlying Öflingen gravel consisted of weathered till originating exclusively from a Black Forest glaciation (Gaar and Preusser 2017). These dates ranged between 19·5 ± 1·8 ka to 68·1 ± 5·9 ka, implying the underlying Alpine gravel pre dates MIS 6. This fits the broader context of the regional glacial history and associated gravel deposits (Preusser 2011), alongside the fascinating history of river capture as the Danube, Aare via the Doubs flowing into the Rhône catchment, and Rhine swapped various portions of their headwaters during the last 4·2 Ma (Yanites et al 2013). Overall, this map shows an intricate pattern of criss-cross faulted bedrock geology. This ranges from Neogene – Paleogene clastic molasse sediments, to Jurassic chalks and marls, and Permo-Triassic sandstones, dolomites, evaporites, chalks and silts. Only faults are projected beneath superficial deposits, rather than like the BGS did showing bedrock boundaries, with under abbreviations identifying superficial deposits, codes for the underlying bedrock units. The Quaternary deposits are subdivided into 43 units, even if the main terraces are grouped together, alongside many symbols including the location of glacial erratics and dolines, plus significant geomorphological features.

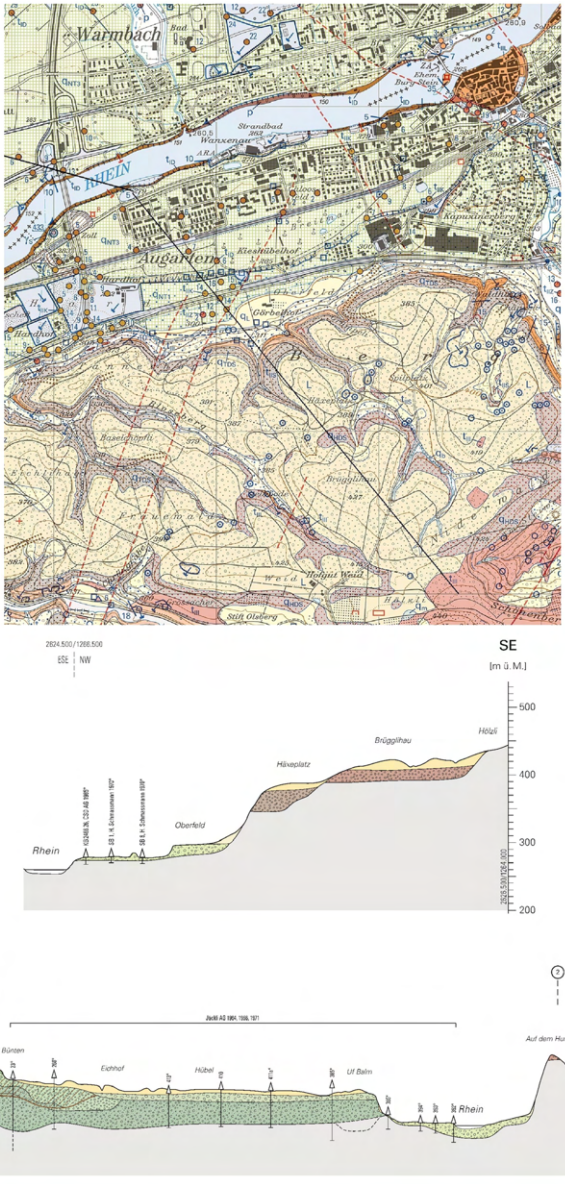

Figure 5a. Extract Sissach - Rheinfelden geological map (Pfirter et al 2019) from historic centre of Rheinfelden built on Triassic Muschelkalk dark brown, with other Triassic sediments t, lighter tones and Permian outcrop along northern river bank p. Section 1 added to map, coloured circles boreholes reaching bedrock below

superficial deposits and depth to this surface in metres, red dashes are faults in underlying bedrock. 5b. Eastern end of plate 2, section 1 through series of river terraces: Early Pleistocene upper gravels light rusty brown and deep gravels light brown, below Löss yellow; light green lower series divided on map into q_{NT1} top level, deposited sometime after the Last Glacial Maximum deposition of q_{NT3} lower level; q_L weathered loam and slope deposits light yellow. 5c. Section 3 elsewhere on this sheet through Möhliner moraine, small patch of Bünten Till at SW end and Bünten quarry, brown diagonal lines extent of glaciotectonic features. Thicker Bünten gravel darker green, Wallbach gravel and Öflingen gravel light green; Zeingen Till above quarry olive, other units same.

Given the extent of the superficial deposits around Zürich airport, the Bülach 25k sheet (1071) has 13 cross sections printed on two large plates, plus a 50k map neatly showing the elevation of the underlying bedrock and position of these profiles (Haldimann *et a.l* 2017). The district had numerous glacial advances during the Middle and Late Pleistocene when deep basins and channels were formed and filled with complex sequences of later deposits. This includes the Glattal depression, partly covered by this extract (Fig 6a) and SW to NE profile showing how it is filled with two different tills and lacustrine deposits (Fig 6b). During the end of the last ice age, the ice marginal lake which formed was up to 40 m deep and rapidly filled with sediment within a few hundred years. The valleys stratigraphy has been placed into nine erosional and depositional cycles, correlated with Marine Oxygen Isotope stages and earlier patterns of regional glaciation (Buechi *et al*. 2018). Around Oberweningen (Fig 7a), the narrower Wehntal gully was probably formed during MIS 8 is also notable (Fig 7b), as about 2 km to the west Mammoth bones were found in a gravel pit on the outskirts of Niederweningen in 1890, with more material discovered during the construction of a housing development in 2003 (Furrer *et al*. 2007). These latest remains were found in a layer formed during Interstadial MIS 3 with bones ^{14}C dated to around 45 ka.

The surrounding 25k maps are of varying quality, and Wohlen (1090) published in 1966 really could do with an overhaul. Since then, our interpretation of superficial deposits has been greatly enhanced, so the key to 168 Hitzkirch (1100) to its south has much more clearly structured Quaternary units, alongside refined geomorphological features (Gubler 2020). The memoir includes a revised cross-section from an unpublished report, showing a cross section through a terminal moraine (Fig 8), as a good example of the sort of material which can be disseminated by formal publication.

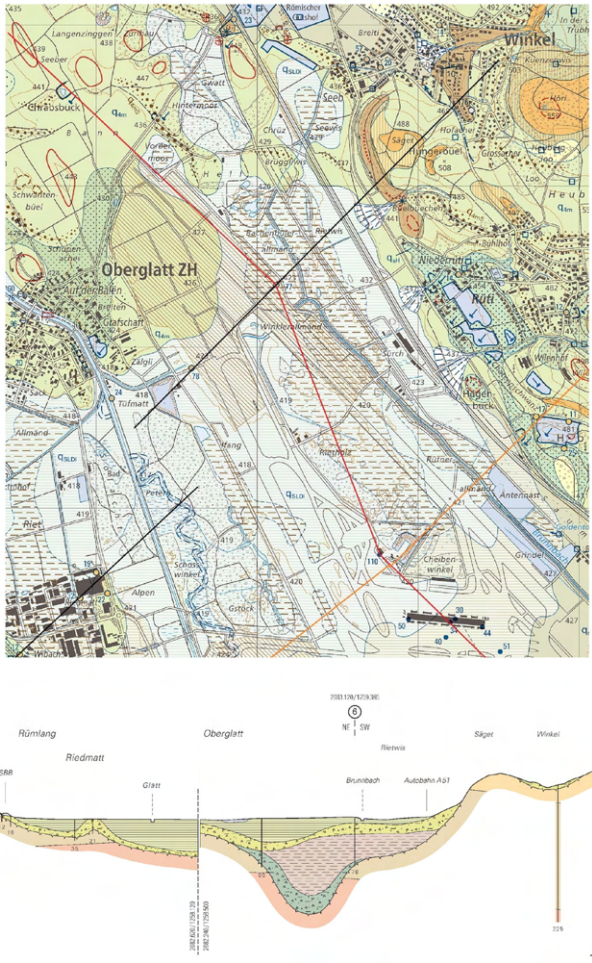

Figure 6a. Extract from Bülach geological map (Haldimann et al 2017) including Oberglatt and Winkel with Late Pleistocene moraines q_{4m} lime green and gravel darker green with dots, plus Middle Pleistocene gravels slighter lighter tone to the east of runways. Red lines circle drumlins, orange and brown indicate Oligocene-Miocene molasse deposits, some of which is covered by glacial tills and subdued by vertical lines. Position of cross sections highlighted, 10 in black, 6 in red, 9 in orange. 6b. Plate 2, section 10 nature of infill within the Oberglatt depression. Middle Pleistocene moraine (till) dark green at base, followed by lacustrine deposits purple; overlain by late glacial moraine (till) lime green, and lacustrine deposits green with horizontal lines; along with nature of underlying bedrock.

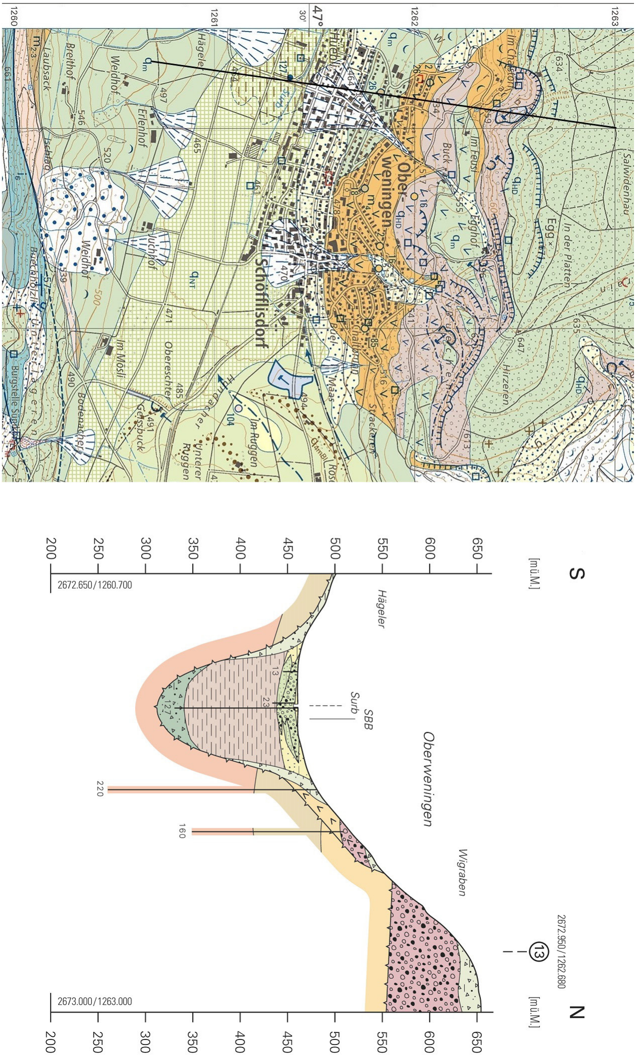

Figure 7a. Extract from Bülach geological map (Haldimann et al 2017) around Oberweningen and Schöfflisdordf with position of Plate 1, section 4 indicated. From top main units: Upper Pleistocene moraines q_m dark green, underlying Early Pleistocene upper gravels q_{HD} purple; V indicate landslips, crescents slipped ground, light yellow with dots slope and solifluction debris, downhill dashes uncoloured debris cones; orange Miocene molasse deposits m_4 orange; Upper Pleistocene lower terrace gravels q_{NT} grided lines green, peat bog superimposed

brown dashes, cambering on southern slopes uncoloured with larger blue dots; Jurassic, Malm i_6 blue; glacial meltwater channels dashes linked by dots headed by arrow, blue lines thrusts dashed beneath superficial deposits. 7b Wehntal gully cross section with borehole through sequence interpreted as follows: down to 10.0 m low terrace gravel, glacier advance (MIS 2 = LGM); to 19.5 m stream and swamp deposits (MIS 3?); to 74.1 m lacustrine deposits upper part warm, below colder conditions (MIS 5?); to 76.4 m glacial lake moraine (advance MIS 6?); to 113.7 m cold lake deposits (MIS 7?); to 125.3 m gravel (withdrawal phase of MIS 8 advance?); to 127.0 m ground moraine (glacier advance MIS 8?), bedrock not reached.

Extent of past ice sheets

In the Jura mountains 172 Le Locle (1143) on the French border (Eichenberger *et al*. 2020), features Neogene - Paleogene clastic molasse outliers, Cretaceous to Jurassic marls, calcareous marls and limestones, which have been subject to complex thrusting, alongside late glacial and post glacial deposits plus geomorphological features. The survey slightly revises the bedrock geology on the Travers (1163) sheet to its south (Nowell 2020), while to it east Val de Ruz (1144) published in 1968 needs remapping. This extract is centred on Le Locle (Fig 9a), the former site of a narrow late glacial lake about 3¼ km long which persisted, until the Maris des Calame was finally drained via an adit under the Col des Roches in the early 19th century. The detrital material deposited in this valley has been subject to detailed study more than a century to produce this profile (Fig 9b). During the Younger Dryas to mid Holocene, this accumulated at around 1 mma^{-1} and dropstones may indicate ice flows existed until the early Preboreal.

During the Last Glacial Maximum - LGM, this district was on the edge of the Jura ice sheet and the memoir includes a revised map based on more recent evidence (Fig 10) than the national map (Bini *et a.l* 2009; Nowell 2014b). This decay and phases of glacial retreat were plotted in more detail on a 50k map immediately to its south (Pasquier *et al*. 2013). This plate shows post LGM Jura ice cover at a more extensive phase than the Cheminot retreat, alongside the maximum extent of the Rhone Glacier and up to six supposed phases of its retreat (Fig 11). Another excellent example of clear and easy to absorb illustrations show the extent of glaciation in the Mendrisio and Como (1373-4) area in southernmost Switzerland, based on extensive Middle and Upper Pleistocene deposits covering wide areas within this district (Bernoulli *et al*. 2018; Nowell in prep). These glacial and fluvio-glacial deposits define both, the Most Extensive Glaciation (MEG) during either marine isotope stage 12 Elsterian = Anglian (424–478 ka) or 16 Cromerian complex (621–676 ka), and LGM which have a more limited extent and could otherwise have been obliterated (Fig 12). During the LGM and the first recessional

phases, ice covered Mendrisiotto from 27.3 to 19.9 ka cal BP. The memoir also includes photographs of erratic boulders and three paleogeographic maps showing the first phases of melting at the end of the LGM around Trévano, Italy.

Photographs documenting glacial retreat

Using archives, it is possible to document the retreat of glaciers, and a good example is about 11 km east of Innerkichen, where the Trift glacier has receded

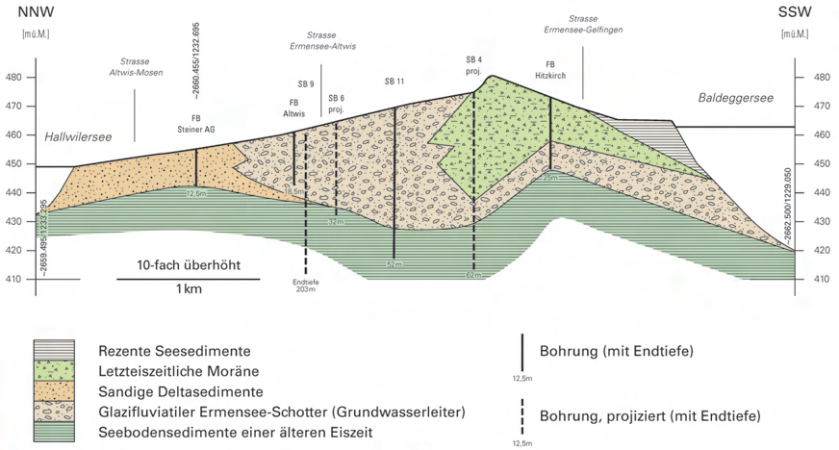

Figure 8. Cross section between Hallwilersee 448 m and Baldeggersee 463 m lake levels which are in hydrological connection via gravels within Ermensee - Hitzkirch terminal moraine from the Bremgarten - Zürich stand. Key: recent sediments; last ice age moraine; sandy delta sediments, glaciofluvial Ermensee gravels (aquifer); older ice age sediments. Solid vertical lines boreholes with terminal depth, dashed lines borehole projected onto the line. Copyright © swisstopo, All rights reserved

by more than 4 km since the end of the Little Ice Age around 1850 (Gisler *et al*. 2020; Steinemann *et al*. 2021). The glacier was described and sketched in 1839, before the first detailed map was published in 1864. This can be viewed using the "Journey through time – topographic maps" layer on the swisstopo website, which allows viewers to select different years to be selected, though a quick left click is required to see the actual year and publication details pop up. By 1929 the tongue of the glacier had already retreated roughly a km, and in 1959 ice still filled the Windegg gorge, at which point a series of photographs taken from the same vantage point shows its dramatic collapse (Fig 13). Given that massive chunks of ice could break off the front of the current glacier into the newly formed

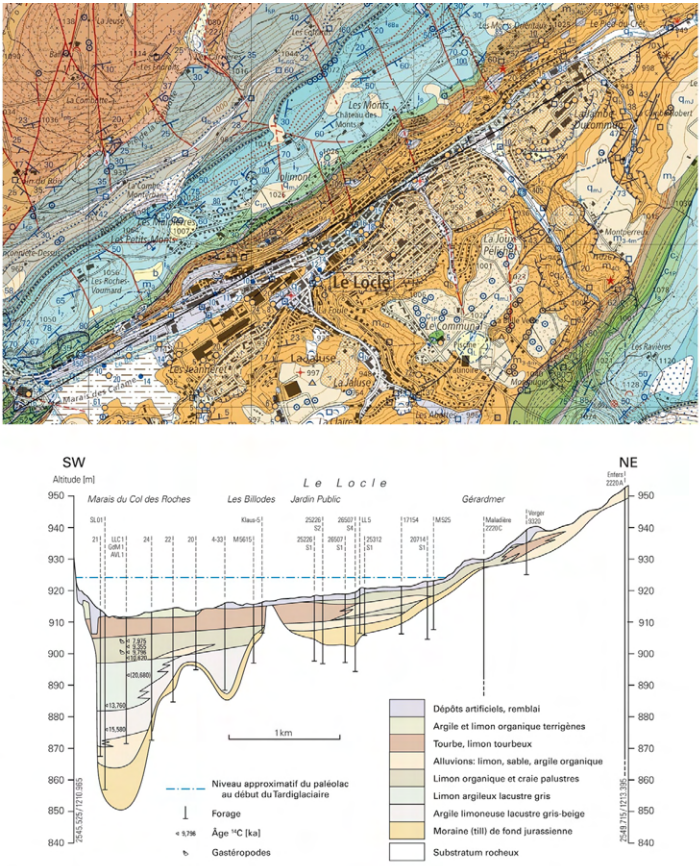

Figure 9a. Extract from Le Locle geological map (Eichenberger et al 2020), position of cross section in Figure 34 indicated. Note town located within a Miocene molasse tectonic outlier, orangey brown, land slipped along SE side of valley - V symbols; surrounded by Cretaceous sediments green tones and Jurassic light green, blue and blue grey brown tones. Blue lines thrusts, red faults, circles with dot in centre dolines, lines with downslope marking back slope features, Marais des Calame drained peat bog, brown dots and dashes. 9b. Profile along valley with former lake level 923-4 m above sea level indicated by dashed line, uncalibrated radiocarbon dates noted, along with gastropods. Key: made ground, purple; clay and loam or organic silt with weathered material, light green, peat with peaty loam, brown; alluvium with loam, sand and organic clay light yellow; organic loam with marsh chalk, olive green; clayey loam grey lake deposits, pallid green; Loamy grey-beige lake clay, light grey; moraine (till) with Jurassic limestone clasts, light brown; uncoloured bedrock.

lake below, geophysical surveys were conducted and automatic cameras set up, to monitor the risk of floodwater flowing into the Gadmertal and presumably down towards Innerkirchen.

Another perspective (Fig 14), is provided via the "Aerial images swisstopo oblique" layer, with numbered squares for the year each photograph was taken, centred on the landscape it captured. By clicking a mini preview pops up in object information, with the link to "More info" including a full screen mode where it is possible to capture them at different degrees of enlargement, rather than ordering full size images from the Geodatenabgabe und analoge Sammlungen. This northward view extends into the upper parts of the Rhône glacier, which was captured from the opposite direction (Fig 15). In 1866 the Rhône glacier was mapped extending around 2□ km further down the valley, at an altitude of ~1,763 m within the Gletschenbode alluvial plain. By the time this aerial photograph was taken, the 50k map published in 1948 put its end at 1,810 m, about a km from its current terminus behind a small proglacial lake with an altitude of 2,208 m. The pioneering

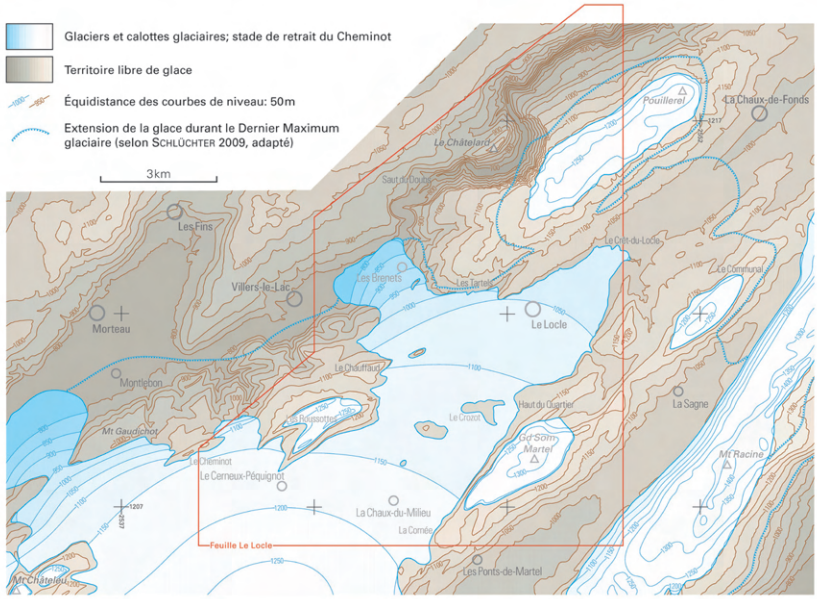

Figure 10. Extent of LGM ice around the Le Locle district shown by blue dots linked by a thin line, with blue tones for the stade associated with the Cheminot retreat, with 50 m contours, and brown tones for ice-free areas during late glacial times. Figure 31, page 84 (Eichenberger et al 2020). Copyright © swisstopo, All rights reserved.

flights which produced these images, started in 1926 with photographs taken by hand from open type Zepp C.II aircraft (History of swisstopo, 2020 download).

The "Terrestrial images swisstopo black and white" layer, provides photographs taken in and around the high Alps for stereo terrestrial photogrammetry, from precisely surveyed baselines until they were replaced by aerial photogrammetry in the 1950s. At first it is confusing clicking squares to get highlighted in yellow the foot print of each image, which pops up within a preview. Then, it is possible to capture images with different enlargements, and download the "Expert data sheet" in German. These are clearly set out, showing where the numbered photographs

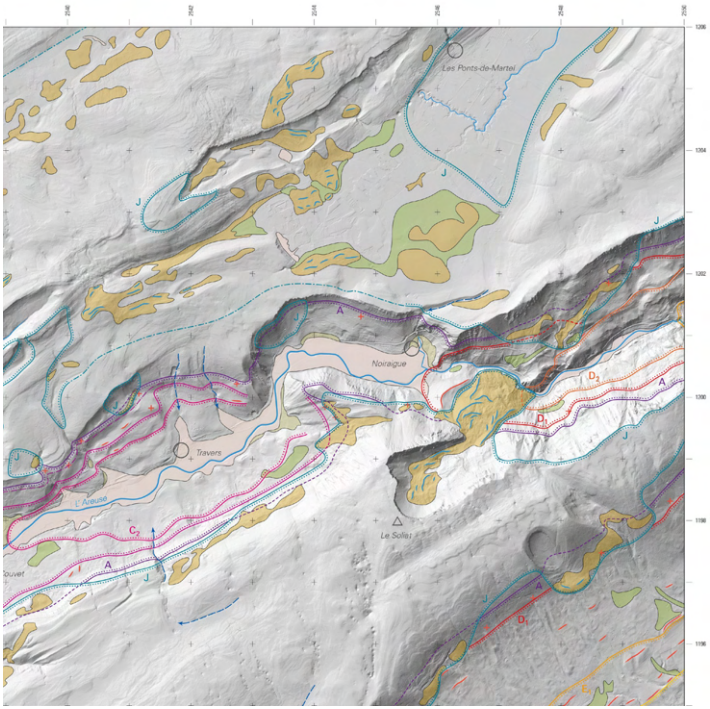

Figure 11. Portion plate 4 Travers (1163) showing extent of LGM Rhône glacier = A, purple line with dots for ice on that side, B to E = different stages of post LGM retreat outlined in different colours, J = extent of post LGM Jura ice cover, draped on synthetic topographic image revealing geomorphological features within the landscape (Pasquier et al 2013). Red cross, Rhône ice erratic blocks above 880 m altitude; red and blue lines, moraines associated Rhône and Jure ice respectively; dashes tipped with an arrowhead, dry side valleys formed by meltwater from Jura glaciers. Brown, moraine (till) deposited by Jura ice, green fluvial glacial sand and gravel, light green deltaic sand and gravel, light grey alluvium and lake deposits. Copyright © swisstopo, All rights reserved

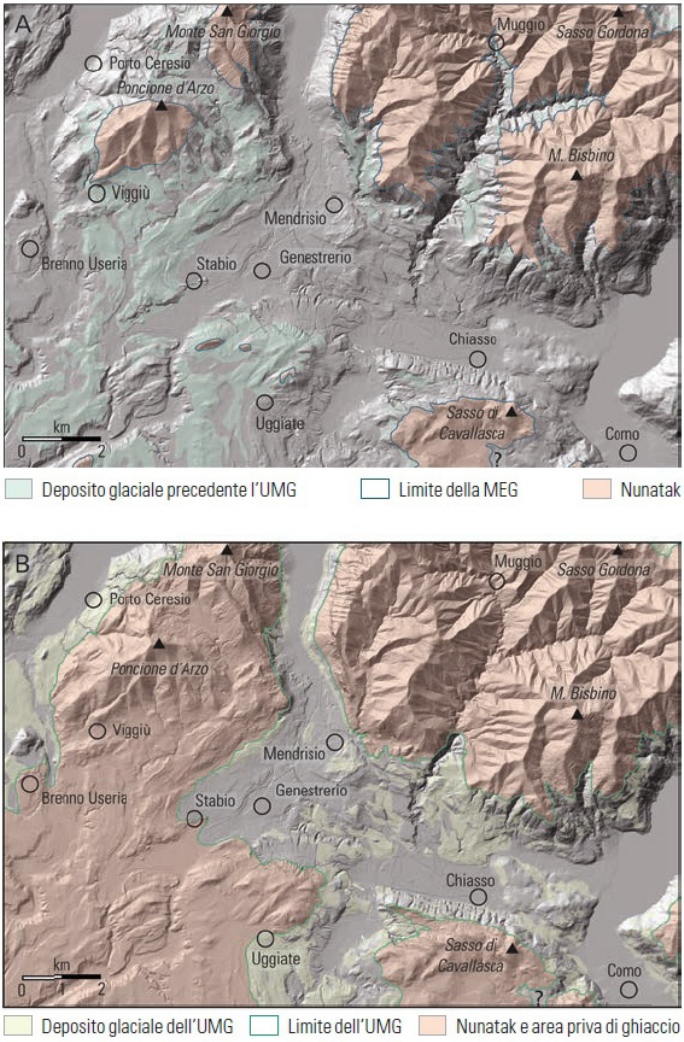

Figure 12. Mendrisio and Como district with areas covered by ice in grey and related deposits light green with ice free ground in brown: **A**, during Most Extensive Glaciation (MEG); **B**, Last Glacial Maximum (UMG). Figure 27 Mendrisio-Como memoir (Bernoulli et al 2018). Copyright © swisstopo, All rights reserved

from each baseline were taken.

During 1926 and 27 the Grosser Aletschgletscher (Great Aletsch glacier) was photographed from many perspectives along its entire 23 km length (Fig 16). This was some 3·2 km from where it ends today, though this glacier is still at least a km longer than its assumed mid-Holocene extent (Grämiger *et al*. 2018), before readvances culminated in the Little Ice Age. Naturally, it has been documented for over a century with cartography. Thus, studies documenting how retreat has triggered slope failure in the vicinity of the tongue, as this supporting wedge of ice has been removed by melting, used 1926 mapping as their baseline (Kos *et al* 2016; Storni *et al*. 2020). But this has been done without looking through these

Figure 13. Retreat of the Trift glacier viewed from the north in 1948, 2002, 2006, 2011, 2014, 2019 from the glacier archive and Swiss Alpine Club (Gisler et al 2020). Copyright © swisstopo, All rights reserved

stereographic archives to see what else might be gleaned from these photographs, when they were taken to enhance this topographic mapping. When the future response of the Grosser Aletschgletscher to climate change was modelled (Jouvet and Huss 2019), these simulations were tested against past changes in elevation to check their reliability. Even with local air temperature rises of 1 to 2½°C relative to 1960-1990, it would lose over half its volume and length by the end of the century, just leaving the Konkordiaplatz in place in this optimistic climate scenario (Jouvet and Huss 2019). In addition to ground-based studies, satellite radar can now monitor changes in height and surface velocity across the entire glacier (Leinss and Bernhard 2021).

Conclusions

These brilliant websites could be enhanced with some extra information. The BGS GeoIndex website, separates out layers of geological mapping, but blocks saving extracts with detailed keys generated only for printing. However, in Switzerland this would require plotting uncertain bedrock boundaries underneath superficial deposits. Another blind spot, is the lack of borehole information, unlike the BRGM and BGS websites which include many of these records. Though, they have both stopped publishing maps without making it clear where their digital geological boundaries have since been revised, by putting reports online highlighting these results. The economic benefits of producing geological maps, for the wider benefit of society cannot be overstated when the cost of ignorance is so expensive. HS2 has brought this into the open, "significantly more challenging" ground conditions already adding around £10 bn to the cost of this high-speed railway (Nowell 2021a). With, evermore pressure for development and climate change, continued publication is required to manage resources, planning, flooding and geological hazards like landslips.

Once within about a decade 25k coverage of Switzerland has been completed, at between 600,000 to 800,000 CHf (roughly £470 to 630k) per sheet (Peter Hayoz CGeol, pers comm) covering 210 km^2, there would be a strong case for resurveying earlier maps. In comparison, I was told surveying and publishing a BGS 50k geological sheet cost around £250,000 a decade ago, covering ~559½ km^2, which it turns out was wonderful bargain. This shows what can be done with the right political will in Switzerland, as part of the rational of the swisstopo website continuing to improve the overall quality of their topographically based data, unhindered by excessive copyright. Thus, all sorts of diverse layers have been added, so it is easily possible to analyse them. In contrast, the government owned Ordnance Survey, with a primary focus on revenue protection, has to provide a dividend to the UK Treasury, so that such an open and accessible high quality website would not be feasible. Instead, the Swiss take the view that usually free online data, will boost the economic efficiency of society generating increased

Figure 14. Oblique aerial photo 21 August 1950 when Trift glacier still filled Windegg gorge. View probably extends from around where the glacier terminated around 1850 at an altitude of roughly 1,360 m, near the Triftbahn cable car station, over to the upper glacier and onto Limistock 3,182 m, part of a nunatak ridge between Tieralplistock, 3,382 m to the right obscured by the serial numbers and Wysse Nollen, 3,397 m. In distance, behind this saddle Eggfirm and Grossfirm forming upper portions of Rhône glacier, source of the river Rotten in German.

Figure 15. Oblique aerial photo Rhône glacier 25 August 1945, when it extended down to around 1,810 m. On western flank to left is the Gärstenhoren 3,183 m ridge, then Hintere Gelmerhörner ridge up to Tieralplitock 3,382 m, across the Limistock saddle to Wysee Nollen 3,426 m, up to Eggstock 3,555 m starting eastern watershed, peaks at Dammastock 3,630 m, along this ridge to Galenstock 3,586 m and Chli Furkahorn 3,025 m. Road zigzagging up eastern side above glacier reaches the Furkenpass 2,429 m just out of view.

tax revenues to pay for this enlightened approach. As a result, this has produced a most welcome windfall for Quaternary researchers, lectures, teachers and students seeking high quality material for potential projects, along with encouraging more fieldwork in Switzerland.

Acknowledgements

To Peter Hayoz, Geologist CHGEOLcert, Head of Administrative Unit SGS, Federal Department of Defence, Civil Protection and Sport DDPS, Federal Office of Topography swisstopo, Seftigenstrasse 264, 3084 Wabern, for help explaining how to make best use of the data viewer, answering wider questions about the Swiss Geological Survey and providing high resolution copies of illustrations. Also, Dr Paul Murray, County Cork, Ireland, for trimming and tidying up many of the figures.

Figure 16. Grosser Aletschgletscher near its tongue 19 August 1927, from left of Tyndall base line (642,200 137,489 LV03 grid ref 2,319 m altitude). Then it terminated at around 1,430 m compared to 1,610 m today. The top triangle in image lines up with Eggishorn 2,927 m some 9·6 km away. On the, "Map of potential permafrost distribution" layer its slopes are modelled as being likely to have fairly extensive areas of frozen ground. On left hand side, ice patch flowing down Üsser Aletschji has since melted leaving a recent moraine q_{rm} in Obtliejergand area (Steck 2011). Site of future Moosfluh cable car station, after which rockslides are named (Storni et al 2020), probably just out of view on the opposite side of the valley.

References

Bache, F., Olivet, J-L., Gorini, C., Rabineau, M., Baztan, J., Daniel, A. and Suc, J-P. (2009). Messinian erosional and salinity crises: View from the Provence Basin (Gulf of Lions, Western Mediterranean). *Earth and Planetary Science Letters*. 286, 139-157

Bernoulli, D., Ambrosi, C., Scapozza, C., Stockar, R. Schenker, F.,L., Gaggero, L., Antognini, M. and Bronzini, S. (2018). Foglio 1373 Mendrisio con parte del Foglio 1374 Como, 199 pp. *Atlante geologico della Svizzera 1:25,000, Carta 152*. ISBN 978 3 302 40077 8 Ufficio federale di topografia, CH-3084 Wabern

Bini, A., Buonchristiani, J.-F., Couterand, S., Ellwanger, D., Felber, M., Florineth, D., Graf, H.R., Keller, O., Kelly, M., Schlüchter, C. and Schöneich, P. (2009). *Die Schweiz während des letzteiszeitlichen Maximums (LGM), La Suisse durant le dernier maximum glaciaire, La Svizzera durante l'ultimo Massimo glaciale, Switzerland during the Last Glacial Maximum 1:500,000*. In: Burkhalter, R. (Ed.). Federal Office of Topography, swisstopo, CH-3084 Wabern, Bern.

Buechi, M., Graf, H., Haldimann, P., Lowick, S. and Anselmetti, F. (2018). Multiple Quaternary erosion and infill cycles in overdeepened basins of the northern Alpine foreland. *Swiss Journal of Geosciences*. 111, 133-167

Cohen, D., Gillet-Chaulet, F., Haeberli, W., Machguth, H. and Fischer, U. H. (2017). Numerical reconstructions of the flow and basal conditions of the Rhine glacier, European Central Alps, at the Last Glacial Maximum. *The Cryosphere*, 12, 2,515-2,544

Eichenberger, U., Mojon, P-O., Gogniat, S., Pictet, A., Blant, D., Locatelli, D. Metral, V. and Morard, A. (2020). *Feuille 1143 Le Locle, avec partie de la feuille 1123 Le Russey, 175 pp. Atlas géologique de la Suisse 1:25,000, Carte 172*. ISBN 978 3 302 40103 4 Office federal de topographie, CH-3084 Wabern

Furrer, H., Graf, H. and Mäder, A. (2007). The mammoth site of Niederweningen, Switzerland. *Quaternary International*, 164, 85-97

Gaar, D. and Preusser, F. (2017). Age of the Most Extensive Glaciation of Northern Switzerland: Evidence from the scientific drilling at Möhliner Feld. *Quaternary Science Journal*, 66, er 1-5

Geodesy (2016). *Formulas and constants for the calculation of the Swiss conformal cylindrical projection and for the transformation between coordinate systems*. Federal Office of Topography swisstopo, Seftigenstrasse 264, P.O. Box, CH-3084 Wabern

Girardclos, S., Hilbe, M., Corella, J. P., Loizeau, J. L., Kremer, K., DelSontro, T., Arantegui A., Moscariello A., Arlaud F., Akhtman Y., Anselmetti, F.S. and Lemmin, U. (2012). Searching the Rhone delta channel in Lake Geneva since François Alphonse FOREL. *Archives des Sciences*, 65, 103-118.

Gisler, C., Labhart, T., Spillmann, P., Herwegh, M., Della Valle, G. Trüssel, M. and Wiederkehr, M. 2020. *Blatt 1210 Innerkirchen, 210 pp. Geologischer Atlas der Schweiz 1:25,000, Karte 167*. ISBN 978 3 302 40102 1 Bundesant füf Landestopografie, CH-3084 Wabern

Grämiger, L., Moore, J., Gischig, V. and Loew, S. (2018). Thermomechanical Stresses Drive Damage of Alpine Valley Rock Walls During Repeat Glacial Cycles. *Journal of Geophysical Research: Earth Surface*, 123, 2620–2646

Gubler, T. (2020). Blatt 1110 Hitzkirch, 128 pp. Geologischer Atlas der Schweiz

1:25,000, Karte 168. ISBN 978 3 302 40099 0 Bundesant füf Landestopografie, CH-3084 Wabern

Haldimann, P., Graf, H. R. and Jost, J. (2017). *Blatt 1071 Bülach, 146 pp. Geologischer Atlas der Schweiz 1:25,000, Karte 151*. ISBN 978 3 302 40088 4 Bundesant füf Landestopografie, CH-3084 Wabern

Jordan, P. (2010). Analysis of overdeepened valleys using the digital elevation model of the bedrock surface of Northern Switzerland. *Swiss J Geosci* 103, 375–384

Jouvet, G. and Huss, M. (2019). Future retreat of Great Aletsch Glacier. *Journal of Glaciology*, 65, 1-4

Kos, A., Amann, F., Strozzi, T., Delaloye, R., Von Rütte, J. and Springman, S. (2016). Contemporary glacier retreat triggers a rapid landslide response, Great Aletsch Glacier, Switzerland: Glacier retreat triggers large landslide. *Geophysical Research Letters*. 43, 12,466-12,474

Leinss, S. and Bernhard, P. (2021). TanDEM-X: Deriving In: SAR Height Changes and Velocity Dynamics of Great Aletsch Glacier. *IEEE Journal of Selected Topics in Applied Earth Observations and Remote Sensing*, 14, 4,798-4,815

Leroux, E., Rabineau, M., Daniel, A., Gorini, C., Molliex, S., Bache, F., Robin, C., Droz, L., Moulin, M., Poort, J., Rubino, J-L and Suc, J-P. (2017). High-resolution evolution of terrigenous sediment yields in the Provence Basin during the last 6 Ma: Relation with climate and tectonics. *Basin Research*, 2017, 29, 305-339

Lofi, J. (Ed) (2018). Seismic Atlas of the Messinian Salinity Crisis markers in the Mediterranean Sea – Volume 2. *Mémoires Société Géologique de France*, t. 181 and Commission for the Geological Map of the World, 72 pp., with DVD Rom

Molliex, S., Rabineau, M., Leroux, E., Bourlès, D., Authemayou, C., Daniel, A., Chauvet, F., Civet, F. and Gwenael, J. (2016). Multi-approach quantification of denudation rates in the Gulf of Lion source-to-sink system (SE France). *Earth and Planetary Science Letters*. 444, 101-115

Nowell, D.A.G., Jones, M.C. and Pyle D.M. (2006). Episodic Quaternary volcanism in France and Germany. *Journal of Quaternary Science*, 21, 645-675

Nowell, D.A.G. (2014a). Italian geological maps - Why ending systematic surveys is the ultimate false economy. *Geoscientist*, 24, May, 10-15

Nowell, D.A.G. (2014b). Ice and Glaciers - Switzerland during the Last Glacial Maximum. *Quaternary Newsletter*, 134, 65-68

Nowell, D.A.G. (2020). Book Review - Suisse Jura 1:25,000 geological maps, Travers, Chasseral and Bellelay. *Proceedings of the Geologists' Association*, 131, 233-234

Nowell, D.A.G. (2021a). Geology of Marseilles to Italy high speed TGV railway line compared to HS2 in Britain. *Geology Today*, 37, 23-30

Nowell, D.AG. (2021b). Book Review - Seismic Atlas Messinian Salinity Crisis in the Mediterranean Sea – Vol 2. *Proceedings of the Geologists' Association*, 132, 249-250

Nowell, D.A.G. in prep. Mendrisio, Château-d'Oex and Sargans geological maps of Switzerland, free online data viewer and downloads. *Geology Today*

Pasquier, F., Burkhard, M., Mojon, P-O. and Gogniat, S. (2013). Feuille 1163 Travers, 148 pp. Atlas géologique de la Suisse 1:25,000, Carte 162. ISBN 978 3 302 4068 6 Office federal de topographie, CH-3084 Wabern

Pfirter, U., Jordan, P., Graf, H.R., Pietsch, J. and Huber, M. (2019). Blatt 1068 Sissach, mit Südteil von blatt 1048 Rheinfelden, 212 pp. Geologischer Atlas der Schweiz 1:25,000, Karte 161. ISBN 978 3 302 40100 3 Bundesant füf Landestopografie, CH-3084 Wabern

Preusser, F., Reitner, J.M. and Schlüchter, C. (2010). Distribution, geometry, age and origin of overdeepened valleys and basins in the Alps and their foreland. *Swiss Journal of Geoscience*, 103, 407–426

Preusser, F., Graf, H., Keller, O., Krayss, E., and Schlüchter, C. (2011). Quaternary glaciation history of northern Switzerland. *Quaternary Science Journal*, 60, 282-305

Sastre, V., Loizeau, J.L., Greinert, J., Naudts, L., Arpagaus, P., Anelmetti, F.S., and Wildi, W. (2010). Morphology and recent history of the Rhône River Delta in Lake Geneva (Switzerland). *Swiss Journal of Geosciences*, 103, 33-42

Steck, A. (2011). *Blatt 1269 Aletschgletscher, mit Teil von blatt 1249 Finsteraarhorn, 62pp. Geologischer Atlas der Schweiz 1:25,000, Karte 131*. ISBN 978 3 302 40051 8 Bundesant füf Landestopografie, CH-3084 Wabern

Steinemann, O., Ivy-Ochs, S., Hippe, K., Christl, M. Haghipour, N. and Synal, H.-A. (2021). Glacial erosion by the Trift glacier (Switzerland): Deciphering the development of riegels, rock basins and gorges. *Geomorphology*. 375. 107533.

Storni, E., Hugentobler, M., Manconi, A. and Loew, S. (2020). Monitoring and analysis of active rockslide-glacier interactions (Moosfluh, Switzerland). *Geomorphology*, 371, 107414

Yanites, B.J., Ehlers, T.A., Becker, J.K., Schnellmann, M. and Heuberger S. (2013). High magnitude and rapid incision from river capture: Rhine River, Switzerland. *Journal of Geophysical Research: Earth Surface*, v.118, 1060-1084

Websites

BGS GeoIndex geological maps and UK data.
https://www.bgs.ac.uk/map-viewers/geoindex-onshore/

BRGM geological maps and data for France including overseas departments
http://infoterre.brgm.fr/

Digital Geological maps – follow links to different Swiss series, then scroll down individual listings to trigger downloads
https://www.swisstopo.admin.ch/en/geodata/geology/maps.html

Géoportail – French cartographic data viewer including geological mapping
https://www.geoportail.gouv.fr/carte

Glaciers online – with many well documented examples in Switzerland and around the world
https://www.swisseduc.ch/glaciers/alps/index-en.html

Federal Office of Topography swisstopo - Freely Available Online Tools – online data viewer via links to different starting categories
https://www.swisstopo.admin.ch/en/home/meta/supply-structure/freely-available.html

Free basic geodata (OGD) - Frequently Asked Questions section
- Finance, personnel, law, politics
https://www.swisstopo.admin.ch/en/swisstopo/free-geodata.html

David Nowell
2 Tudor Road
New Barnet
Herts. EN5 5PA
zenadsl5483@zen.co.uk

REPORTS

'JAMES CROLL – FROM JANITOR TO GENIUS'

Online meeting co-sponsored by the Royal Scottish Geographical Society and the QRA

April 16th 2021

After almost 2 years in the planning, but following an idea mooted five years ago, the QRA co-sponsored a bicentenary commemoration of the birth of James Croll (1821-1890) with the Royal Scottish Geographical Society (RSGS). Croll, whose name adorns the QRA's senior medal, was the Perthshire-born, self-taught prodigy who laid the foundations for climate change science. 'James Croll – from janitor to genius' was presented as a whole-day online meeting on 16th April, 2021. Croll was a stonemason's son who became internationally celebrated as a proponent and developer of the astronomical theory of climate change with its implications for glaciation, oceanography and much else. The meeting, with 14 presentations and lively question and answer sessions, explored Croll as a person and as a scientist, with specialists drawn from the worlds of science, history and popularisation.

The programme had two main, but interlocking strands – Croll the man and Croll the scientist. The first was introduced by **Kevin Edwards** (Universities of Aberdeen and Cambridge) who provided a context for the day and demonstrated that although Croll is not a major figure within popular consciousness, there is in fact a wealth of archival and genealogical evidence available with which to inform his biography. In a further talk, he argued that the year 1876, when many academic honours were bestowed on Croll, represented the summit of his scientific life. An informative video on the geographical, historical and scientific influences and achievements of Croll was presented by **Mike Robinson** (RSGS). This gave many viewers the opportunity to see the landscapes in which Croll was brought up and the place in Cargill churchyard where his remains were laid to rest. **Laura Brassington** (University of Cambridge) explored Croll's navigation of scientific societies and reflected upon the degree to which his humble, social background was an impediment to institutional assimilation; it might also have encouraged his engagement with the more meritocratic structures of the Geological Survey of Scotland and the *Philosophical Magazine*. **Diarmid Finnegan** (Queen's University Belfast) examined the interplay of science, metaphysics and Calvinism as drivers

for Croll's beliefs. For Croll, science had to be conducted on metaphysical principles and the cosmos was fully determined by a perfect intellect. In a paper which bridged the humanistic and scientific dimensions of the meeting, **James Fleming** (Colgate College, Maine) suggested that Croll was involved in a personal quest for a general theory of the unity of nature, in which religion, philosophy and science meshed, and that what Darwin did for life forms, Croll accomplished for climate change.

Malcolm Longair (University of Cambridge) charted transitions from the celestial mechanics of classical times. He introduced us to major mathematicians of the late 18th and 19th Centuries and Croll's development and augmentation of the astronomical background to climate change as adopted by Milutin Milankovitch in the 1920s-1930s. He emphasised that although Croll's contributions became diminished for several generations, his novel insights have now been demonstrated to have been basically correct. The perception that Croll was too far ahead of his time for the real depths of his insights to be fully appreciated was taken up by several of the following speakers. **Alastair Dawson** (University of Dundee) analysed the oceanographic contribution of Croll, demonstrating that, true to form, he had calculated from first principles the quantities of heat delivered by ocean currents to high latitude areas, producing numerous far-sighted ideas. Acting as James Croll's *alter ego*, **David Sugden** (University of Edinburgh) showed how the pioneer's modelled estimates of the Antarctic ice sheet and its dimensions were not improved upon until John Glen developed a realistic flow law for ice some three quarters of a century later. Furthermore, Croll is to be admired for his use of a systems approach in the search for scientific understanding.

James Rose (Royal Holloway, University of London) considered the differing perspectives of Charles Lyell, the Geikie brothers (Archibald and James) and Croll, regarding terrestrial glacial sediments and landforms. He argued persuasively that Croll may have been a reluctant geologist, but that he was a very good one. Indeed, he was influenced by a relatively unacknowledged 'Glasgow School' of glacial geologists, while also sharing in the development of land-ice glacial theories as exemplified particularly by James Geikie. In a presentation by **Chronis Tzedakis** (University College London) on behalf of himself and **Eric Wolff** (University of Cambridge), it was revealed how Croll understood the significance of interglacial deposits in furnishing evidence for multiple glaciations, while the marine sedimentary record was able to deliver a test of astronomical theories as outlined by both Croll and later by Milankovitch, a century after the publication of Croll's monumental 1875 book *Climate and Time in their Geological Relations*. Feedback mechanisms in the Earth system were the focus for **Roy Thompson** (University of Edinburgh), who explained how Croll's fundamental recognition of this concept foreshadowed global warming. This, however, was one of a series of legacy issues embraced by Croll and covering an astonishing range of topics relevant to climate and wider environmental science.

Jo Woolf (RSGS) and **Mike Robinson** (RSGS) explored ways to popularise Croll. Their contributions included a broad spectrum of actual and potential events from seminar- and theatre-based presentations, to publications, exhibitions, and educational tourist trails. It was an opportunity for expression and creativity in a manner which reminds us that Croll was once a young lad, 'full of fun and frolic', who might be opened up to interpretation by people of different ages and backgrounds – a great scientist who was not deterred by impediments of health, early education and social mores.

It had been hoped to hold the meeting in Perth as an in-person event. Sadly, coronavirus put paid to that notion and a Zoom-based event was substituted. Nevertheless, perhaps it is testament to Croll, the speakers and those attending, that the meeting held on to a substantial audience. Gratifyingly, the EventBrowse conference platform informed us that they had selected the event as one of their featured *Editor's List* items for the European time zone. The papers upon which the presentations were based, many of which have been the subject of research conducted especially in connection with the meeting and its publication, will appear in a forthcoming special issue of *Earth and Environmental Science Transactions of the Royal Society of Edinburgh*. The RSGS and QRA, along with the Royal Society of Edinburgh, are to be congratulated for their support of an event in memory of an exceptional man with enduring relevance.

Kevin J. Edwards
Departments of Geography & Environment and Archaeology
School of Geosciences
University of Aberdeen

McDonald Institute for Archaeological Research and Scott Polar Research Institute
University of Cambridge
kevin.edwards@abdn.ac.uk

BOOK REVIEWS

A PRACTICAL GUIDE TO THE STUDY OF GLACIAL SEDIMENTS (SECOND EDITION)

Edited by David J.A. Evans and Douglas I. Benn
QRA, 368 pp.

Available online at https://www.qra.org.uk/technical-guides/

The first edition of this book, edited by Dave Evans and Doug Benn, and published in 2004, has proven to be a key point of reference for, and frequent field companion of, many glacial geomorphologists and sedimentologists over the last 17 years. Glacial sedimentology is a complex and potentially daunting topic: glacial sediments encompass so many depositional environments (e.g. marine, fluvial, lacustrine, aeolian) that an all-round understanding of sedimentology is critical even for the most basic of interpretations. Therein lies the key strength of this book: its ability to set out a range of practical approaches to break down this complexity into a series of manageable chunks and frameworks for analysis. It does this without losing the authoritative confidence typified by the editors' other major stalwart *Glaciers and Glaciation*.

The introductory chapter nicely summarises the scientific method with respect to glacial sedimentology, and prepares the reader with the philosophy required to undertake sedimentological analysis. There then follow seven chapters on how to conduct different types of sedimentary analysis, rounded off by an elegant case study (Drumbeg, Scotland) that draws on many of the methods explained in the previous chapters to provide a description and interpretation of a real glacial sedimentary environment. This transition from theory to practice is a nice way to illustrate how the knowledge gleaned from different approaches can be drawn together to weave a robust reconstruction, and will be particularly useful for students and other workers embarking on a sedimentological project for the first time.

The second edition, newly published jointly by the QRA and the GLWG (Glacial Landsystems Working Group) keeps the chapter structure the same, but goes into a greater level of detail, as indicated by the increase in length from 266 to 375 pages. As a result, it is physically larger than the first edition, with an a-axis of 24 cm (1st edn. 23.4 cm), b-axis of 16.5 cm (1st edn. 15.5 cm) and c-axis of just over 18 mm (1st edn. 10 mm), thus placing it firmly between 'slabs' and 'elongates' on a clast shape ternary diagram (see page 109 for details). Another significant update is that the second edition is now printed in colour throughout (the first edition was in black and white, with a section of colour plates at the back).

The phi and Wentworth grain size classifications are conveniently summarised on the inside of the back cover, as they were in the first edition, but with a new

table extending size classifications beyond boulders to megaliths of hundreds to thousands of km in length. The inside front cover is rejigged with refreshed sphericity and roundness exemplars, and quantified sorting charts. It also includes schematic examples of different types of cross-stratification, which will be a useful go-to reference in the field. To make space for these changes, the visual indicators of grain size and percentage area are removed.

The chapters retain their original authors, but with a few new additions in some of the areas that have been more significantly revised. The authors of each chapter have substantial expertise in the respective sub-discipline and the writing is clear and informative for a wide audience from students to seasoned practitioners throughout. Some small progress has been made in the diversity of the authorship, but this remains an area that lags behind other disciplines.

The illustrations in the 2nd edition are markedly improved, in both quality and number. There are some very useful annotated images that help to explain procedures such as clast fabric analysis that are not necessarily intuitive, which will be helpful to those embarking on this for the first time, and as an aide to those teaching these skills. Likewise, the collection of exemplar photographs helps to train the mind to recognise the plethora of sedimentary structures observable in nature. There are also a good number of images showing examples of how data can be presented, which again will help to train those new to the discipline (and perhaps those with more experience!) how they may present their data to maximise clarity and ease of interpretation.

Throughout the book a number of case studies are used, and there are more of these in the 2nd edition, which also provides some more recent examples. The information and content in each chapter is updated. Chapter 7 in particular (particle lithology and mineral and geochemical analysis) includes some more substantial revision, including some more of the basics of rock and mineral identification. This is a welcome update, particularly since students come to glacial sedimentology from a range of backgrounds and may not be familiar with many rock/mineral types. In the UK for example this is often the case with Geography students.

All in all, the first edition of this book was very popular for very good reasons, providing a wealth of information and practical advice helping a wide range of practitioners to navigate their way through the nuanced world of glacial sedimentology. The second edition cements this (pun intended), and goes further to make this knowledge even more accessible. Thoroughly recommended.

Rob Storrar
Department of the Natural and Built Environment
Sheffield Hallam University
City Campus, Howard Street
Sheffield, S1 1WB
r.storrar@shu.ac.uk

MAMMOTHS AND NEANDERTHALS IN THE THAMES VALLEY: EXCAVATIONS AT STANTON HARCOURT, OXFORDSHIRE

By Katharine Scott and Christine M Buckingham

ArchaeoPress, Oxford, xvii + 251 pp.

Available online at https://www.archaeopress.com/ArchaeopressShop/Public/download.asp?id={79CF52B8-EA8D-4F35-B263-908202643928}

The Stanton Harcourt Channel, exposed by gravel extraction in 1989, led to ten years of excavation by the authors of this significant monograph. At Dix Pit, close to the village of Stanton Harcourt in Oxfordshire, the shallow (1 m) channel is cut into Oxford Clay and underlies the Summertown-Radley (second) terrace of the Upper Thames. With abundant remains of large vertebrates, molluscs, insects and plant remains, Stanton Harcourt provides the most complete available palaeoenvironmental picture of life in southern Britain during the MIS 7 interglacial, as well as the context for the hominins whose presence is recorded in a small but significant collection of artefacts. The mollusc, insect and plant remains clearly indicate an interglacial climate, with marker species consistent with other UK sites referred to MIS 7. A varied biome is reflected by temperate woodland flora combined with a predominantly grazing mammal fauna (mammoth, horse, bison) suggesting grassland close to the catchment. This diversity of habitats is equally reflected in the mollusc and insect faunas. An age pre-dating the last interglacial was suggested by early AAR, ESR and OSR work, and more recent AAR studies by Kirsty Penkman and colleagues place the channel fill late in MIS 7 within the context of the British sequence; overlying cold-stage gravels (complete with ice-wedge casts that penetrate the channel) map as MIS 6 in the Upper Thames sequence.

The authors recognise that organic remains in river deposits often accumulated over long periods of time, and/or are the result of reworking from older deposits, so that their contemporaneity and hence palaeoecological and biostratigraphic significance is limited. At Stanton Harcourt they had the unusual opportunity to excavate, in archaeological mode from top down, an area of some 100 x 150 m that remained available to them over a long period. Based on a forensic three-dimensional bed-by-bed analysis of stratigraphy and sedimentology, as well as the preservational condition and orientation of the enclosed bones, wood, shells and stone tools, the authors make a convincing argument that a significant proportion of the flora, fauna and artefacts were found at or close to their site of original deposition and were contemporaneous with one another.

The channel fill is mostly gravel, with sand and silt lenses. Lower-energy sediments are recorded close to margins, with higher-energy deposits in or close to the 'thalweg'. The authors describe in great detail the composition and sedimentary context of five major bone accumulations in the Stanton Harcourt Channel. Particularly instructive is a photograph of a meander in the modern river Edenlode (Oxfordshire) marking analogous positions of proposed depositional sites of each of these contexts. In one case, fossiliferous sediments accumulated on a point bar on the inner side of a meander bend, interpreted as a result of lateral accretion. There, large bones and tusks frequently rest on finer-grained deposits with their enclosing gravel likely deposited during a subsequent seasonal flooding event. In another instance, a mammoth skull and associated bones are positioned at the outer edge of the channel where it had likely undercut its bank; an oak trunk with roots in life position was found close by.

While some of these bones show signs of river transport, many do not. Partial mammoth carcasses whose disposition matches that seen in recently-deceased elephants today strongly suggest they are at or very close to location of death. Elephants frequently seek water when close to death and may die in a river channel, or carcasses of animals dying close to the river bank would fall or be washed into the channel. Imbrication of larger bones, tusks, wood and reworked *Gryphaea* shells, observed throughout the site, would have made it more difficult for even faster currents to pick them up and transport further. The finds also include clusters of perfectly-preserved bivalves (*Corbicula* and *Potomida*) with articulated valves in upright position, indicating not only autochthony but rapid burial. The study, finally, demonstrates how accumulations of large bones and wood themselves influence subsequent sedimentation.

The most striking feature of the Stanton Harcourt finds is the extraordinary number of mammoth remains recovered – some 100 complete tusks, a further 100 partial tusks, nearly 200 molar teeth (many still in mandibles and skulls) and over 500 postcranial bones. This represents by far the largest single-site sample of mammoth remains from any UK site, and one of the largest in Europe. As such the extensive measurement and photographic data provided by the authors provides a benchmark for future research. Study of this material in comparison with mammoths from other UK sites (Lister & Scott, in prep.) moreover indicates that the Stanton Harcourt mammoths represent a unique form that is similar to the small mammoths from other MIS 7 sites referred to a late form of the 'steppe mammoth' *Mammuthus trogontherii*, but that with shoulder heights of 2.2-2.9 m they are even smaller than those from other sites (such as Ilford, Essex), and in their dental morphology are edging toward the condition seen in the woolly mammoth (*M. primigenius*) that replaces them in MIS 6. This conforms to their likely age toward the end of MIS 7, and the highly consistent form of the Stanton Harcourt molars is further suggestive of their deposition over a relatively short interval.

Within the monograph, the large mammoth sample has enabled a detailed

taphonomic assessment of the preservation potential of different skeletal elements by size, shape and weight. Metric studies of tusks and pelvic bones indicate approximately equal representation of males and females, while dental ageing indicates an adult-dominated assemblage. The authors discuss plausible explanations for the shortage of juveniles, including greater susceptibility to rapid scavenging on the bank, and smaller body parts being more likely transported away by currents once in the river. More speculatively, the position of the deposits at the very end of MIS 7 might signal environmental stress that could account for both low birth rate and small body size. However, this is not evident in the rich palaeoenvironmental profile, and the insects indicate only slightly enhanced seasonality (January mean -2 to +2 C). Seasonality is also indicated in cyclical $\delta^{18}O$ values in bivalve shells, with similar temperatures to those estimated from the insects, so that species such as the bivalve *Corbicula fluminalis* were living close to the edge of their climatic tolerance.

The excavations yielded a total of 36 artefacts, including 15 handaxes (11 flint and 4 quartzite) plus assorted flakes, cores and debitage. All are illustrated in multiple views, together with others from nearby pits in the same channel. Many are in sharp (unrolled) condition, and the detailed stratigraphy indicates that they were deposited under much the same conditions as the bones and wood, such as in shallow depressions within the surface of a point bar, perhaps discarded there when the bar was exposed. Likely sources of raw material are identified, some 20 km distant from the site. In an interesting personal communication by Nick Ashton, it is noted that the absence of Levallois technology stands in distinction from MIS 8 to 7 localities in the Lower and Middle Thames Valley, East Anglia and the south coast. The handaxe industry at Stanton Harcourt is however matched at similar-age sites in the west of England and Wales, suggesting regional differentiation of populations and/or cultural traditions. More speculatively the authors suggest that an upside-down mammoth skull, well-preserved except for a damaged upper part, might have been upended by the hominins and smashed to access the brain; stone tools were found close by and the skull rests on two large pieces of wood that might have been used as levers, a strikingly similar situation to that seen with an elephant skull at the Lower Palaeolithic site of Gesher Benot Ya'aqov, Israel.

This book has been very attractively produced by ArchaeoPress, on high-quality paper with abundant and excellently-reproduced photographs and diagrams of fauna, artefacts and site stratigraphy. These are complemented by engaging artwork reconstructions by the senior author. The volume is in a handy B5 paperback format, far from the classic doorstop monograph, and is also freely available online. The authors express their regret that several of the specialists who worked on the finds (David Keen on molluscs, Russell Coope on insects, Derek Roe and Terry Hardaker on artefacts) are no longer with us, but the long duration of the excavation and work-up meant that they and others had published

their work or provided manuscript reports, and these are worked into the narrative seamlessly but with fulsome acknowledgement, so that the volume has the feel of a coherent narrative. It is a model of detailed research in a depositional context that normally allows only a crude level of recovery and analysis.

Adrian Lister,
The Natural History Museum,
London SW7 5BD
a.lister@nhm.ac.uk

QUATERNARY RESEARCH ASSOCIATION

The Quaternary Research Association is an organisation comprising archaeologists, botanists, civil engineers, geographers, geologists, soil scientists, zoologists and others interested in research into the problems of the Quaternary. The majority of members reside in Great Britain, but membership also extends to most European countries, North America, Africa, Asia and Australasia. Membership (currently *c.* 1,200) is open to all interested in the objectives of the Association. The annual subscription is £20 with reduced rates (£10) for students and unwaged members and an Institutional rate of £35.

The main meetings of the Association are the Field Meetings, usually lasting 3–4 days, in April, May and/or September, a 2-3 day Discussion Meeting at the beginning of January. Short Study Courses on techniques used in Quaternary work are also occasionally held. The publications of the Association are the *Quaternary Newsletter* issued in February, June and October; the *Journal of Quaternary Science* published in association with Wiley; and the QRA Field Guide and Technical Guide Series.

The Association is run by an Executive Committee elected at an Annual General Meeting held during the Annual Discussion Meeting in January. Current officers of the Association are:

President: ***Professor Simon Lewis***, School of Geography, Queen Mary University of London, London E1 4NS (email: president@qra.org.uk)

Vice-President: ***Professor Jane Hart, Department of Geography and*** Environmental Science, University of Southampton, University Road, Southampton, SO17 1BJ. (email: vice_president@qra.org.uk)

Secretary: ***Dr Helen Roe,*** School of Natural and Built Environment, Queen's University Belfast, University Road, Belfast, BT7 1NN, Northern Ireland. (e-mail: secretary@qra.org.uk)

Publications Secretary:
Dr Katherine Selby, Environment Department, Wentworth Way, University of York, Heslington, York, YO10 5NG
(email: publications@qra.org.uk)

Treasurer: ***Dr Rupert Housley,*** Department of Geography, Royal Holloway of London, Egham Hill, Egham TW20 0EX
(e-mail: treasurer@qra.org.uk)

Editor, Quaternary Newsletter:
Dr Sarah Woodroffe, Department of Geography, Durham University, Lower Mountjoy, South Road, Durham, DH1 3LE.
(e-mail: newsletter@qra.org.uk)

Editor, Journal of Quaternary Science:
Professor Neil Roberts, University of Plymouth, Portland Square, Drake Circus, Plymouth, Devon PL4 8AA (e-mail:editor@qra.org.uk)

Publicity Officer: ***Dr Christopher Darvill,*** Geography, School of Environment, Education and Development, The University of Manchester, OxfordRoad, Manchester M13 9PL
(e-mail: publicity@qra.org.uk)

All questions regarding membership are dealt with by the **Secretary**, the Association's publications are sold by the **Publications Secretary** and all subscription matters are dealt with by the **Treasurer**.

The QRA home age on the world wide web can be found at: http://www.qra.org.uk

Registered Charity: 262124

QN

OCTOBER 2021 No. 154

ISSN 0 143-2826